Canadian Journal of
Earth Sciences

OPEN ACCESS | Article

Calibrating geologic strata, dinosaurs, and other fossils at Dinosaur Provincial Park (Alberta, Canada) using a new CA-ID-TIMS U–Pb geochronology

David A. Eberth[a], **David C. Evans**[b], **Jahandar Ramezani**[c], **Sandra L. Kamo**[d], **Caleb M. Brown**[a], **Philip J. Currie**[e], and **Dennis R. Braman**[a]

[a]Royal Tyrrell Museum of Palaeontology, Box 7500, Drumheller, AB T0J 0Y0, Canada; [b]Department of Ecology and Evolutionary Biology, University of Toronto, Toronto, ON M5S 3B2, Canada; [c]Department of Earth, Atmospheric and Planetary Sciences, Massachusetts Institute of Technology, 77 Massachusetts Avenue, Cambridge, MA 02139, USA; [d]Jack Satterly Geochronology Laboratory, Department of Earth Sciences, University of Toronto, 22 Russell St., Toronto, ON M5S 3B1, Canada; [e]Department of Biological Sciences, University of Alberta, Edmonton, AB T6G 2R3, Canada

Corresponding author: **David A. Eberth** (email: deberth@cciwireless.ca)

Abstract

The 100 m thick stratigraphic section exposed at Dinosaur Provincial Park (DPP; southern Alberta) contains bentonites that have been used for more than 30 years to date DPP's rocks and fossils using the K–Ar decay scheme. Limited reproducibility among different vintages of K–Ar and $^{40}Ar/^{39}Ar$ ages inhibited the development of a high-resolution chronostratigraphy. Here, we employ and further test a recently completed U–Pb geochronology and associated age-stratigraphy model to update temporal constraints on the Park's bentonites, formational contacts, and other markers. In turn, we document rock accumulation rates and calibrate ages and durations of informal megaherbivore dinosaur assemblage zones and other biozones. Weighted mean $^{206}Pb/^{238}U$ ages from five bentonites range from 76.718 ± 0.020 to 74.289 ± 0.014 Ma (2σ internal uncertainties) through an interval of 88.75 m, indicating a duration of ∼2.43 Myr and an overall rock accumulation rate of 3.65 ± 0.04 cm/ka. An increase in rate above the Oldman–Dinosaur Park formational contact conforms to a regionally expressed pattern of increased accommodation at ∼76.3 Ma across Alberta and Montana. Palynological biozone data suggest a condensed section/hiatus in the uppermost portion of the Oldman Formation. Dinosaur assemblage zones exhibit durations of ∼700–600 kyr and are significantly shorter than those in the overlying Horseshoe Canyon Formation. A decreased rate in dinosaur assemblage turnovers in the last eight million years of the Mesozoic in western Canada may be explained by withdrawal of the Western Interior Seaway and the expansion of ecologically homogenous lowlands in its wake.

Key words: dinosaurs, geochronology, Dinosaur Provincial Park, stratigraphy, Campanian, Alberta

Introduction

Dinosaur Provincial Park (DPP; the Park), a small geographic area (80 km^2) in southern Alberta, Canada (Fig. 1), yields a rich and uniquely diverse assemblage of Late Campanian vertebrates, including non-avian dinosaurs. The Park is famous for abundant articulated and associated fossil skeletons and bonebeds that contribute to our understanding of peak dinosaur diversity during the Late Campanian and patterns of latitudinal variation in dinosaurian megaherbivore taxa across the Western Interior Basin (WIB) of North America (Lehman 1997, 2001; Currie and Koppelhus 2005, and papers therein; Barrett et al. 2009; Sampson et al. 2010; Gates et al. 2012; Eberth 2015; Ramezani et al. 2022; Roberts et al. 2005, 2013).

Starting in the middle of the 1980s, and continuing episodically for ∼25 years, attempts were made to date DPP's bentonites employing standard and high-precision potassium–argon-system techniques during a time of technological innovation and improvement (Thomas et al. 1990; Eberth and Deino 1992, 2005; Eberth et al. 1992, 2013*b*; Eberth 2005). Although the original K–Ar and $^{40}Ar/^{39}Ar$ radiometric ages published in the 1990s allowed researchers to approximate the ages of the Park's formational boundaries and fossil occurrences (Thomas et al. 1990; Eberth and Hamblin 1993; Eberth 2005, 2017; Ryan and Evans 2005; Mallon et al. 2012; Eberth et al. 2013*a*), there were serious limitations to the reproducibility of those age data. These were in part due to limited accuracy of mineral standard ages and K decay constants used in $^{40}Ar/^{39}Ar$ geochronology, as well as incompatibility of laboratory analytical protocols (see summary in Ramezani et al. 2022). In turn, these limitations inhibited the development of a single comprehensive chronostratigraphy for the Park's strata and fossils.

Fig. 1. Localities of dated bentonites at Dinosaur Provincial Park. (A) Location of Dinosaur Provincial Park in southern Alberta. (B) Map of Dinosaur Provincial Park (shading) and its boundary relative to the Red Deer River. Red dots indicate bentonite sampling locations. Universal Transverse Mercator grid and other outlines from 1:50 000 scale topographic maps produced by the Department of Energy, Mines, and Resources, Government of Canada (NAD83). (C) Google-Earth-Pro (version 7.3.6.9345) satellite image of Dinosaur Provincial Park. Location of measured section (Fig. 2) in yellow. Bentonite localities in red. Imagery date 10 October 2022; © 2023 Maxar Technologies; © 2023 CNES/Airbus. Abbreviations: b, base; BB, Bearpaw Bentonite; FSB, Field Station Bentonite; JCB, Jackson Coulee Bentonite; LCZB, Lethbridge Coal Zone Bentonite; mE, meters east; mN, meters north; N, north; PT, Plateau Tuff; t, top.

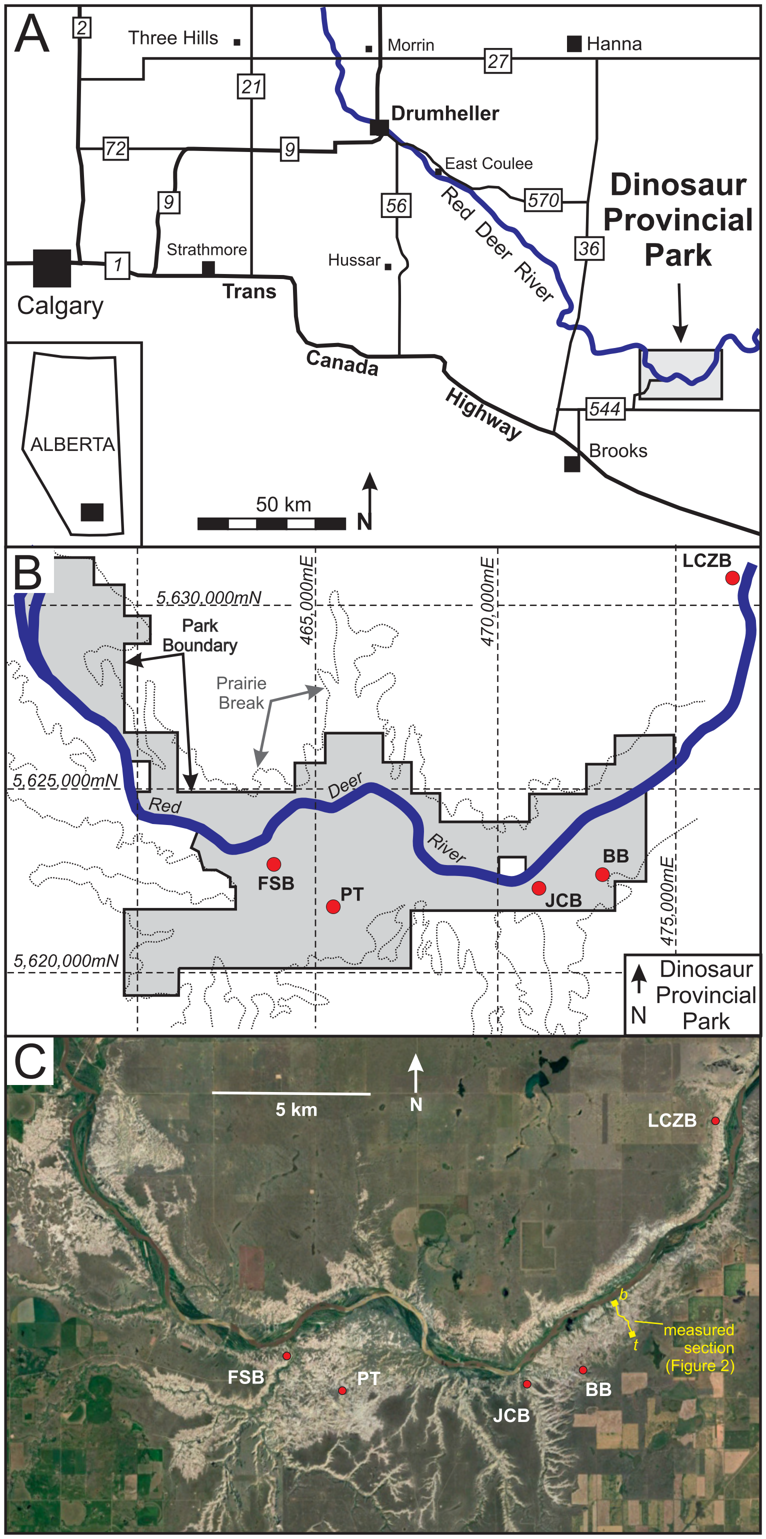

The chemical-abrasion–isotope-dilution–thermal-ionization-mass-spectrometry (CA-ID-TIMS) method of U–Pb zircon geochronology has significantly improved the precision and accuracy of radioisotopic dating applied to the stratigraphic record (e.g., Bowring et al. 2006) and is now regarded as one of the most reliable means with which to build high-resolution and, most importantly, reproducible geochronologies for Mesozoic nonmarine strata (e.g., Cúneo et al. 2013; Ramezani et al. 2014, 2022; Clyde et al. 2016; Gastaldo et al. 2018; Eberth and Kamo 2019, 2020; Zhang et al. 2021; Beveridge et al. 2022). Ramezani et al. (2022) recently published results of their coordinated CA-ID-TIMS U–Pb geochronology project involving Campanian-age dinosaur sites in the WIB of North America, including five bentonites at DPP. Precise and reproducible ages for multiple bentonites at DPP now allow us to revise and calibrate the ages of the Park's formational contacts, rates of rock accumulation, and biostratigraphic zonations. Demonstrated interlaboratory reproducibility of the new geochronology enables future researchers to refine the chronostratigraphy of the Park's dinosaur-rich section through additional U–Pb CA-ID-TIMS geochronology and to correlate the section meaningfully with other dinosaur-rich strata beyond the limits of the Park.

Geologic and paleontologic context

DPP is dominated by exposures of the upper Belly River Group (BRG), an eastward-thinning, nonmarine-to-paralic clastic wedge that interfingers with marine shales of the Western Interior Seaway (WIS). It was deposited in the distal foredeep of the WIB during the middle to late Campanian (Eberth and Hamblin 1993; Jerzykiewicz and Norris 1994; Hamblin and Abrahamson 1996; Hamblin 1997; Eberth 2005; Eberth and Kamo 2020) and accumulated in response to a complex history of tectonic uplift and erosion related to the long-term docking and suturing of accretionary terranes along the western margin of Canada (Cant and Stockmal 1989; Eberth and Hamblin 1993; Price 1994; Hamblin 1997).

The BRG section (outcrop and subsurface) at the Park is approximately 280 m thick and, in ascending order, consists of the Foremost (∼160 m), Oldman (∼40 m), and Dinosaur Park (∼80 m) formations (Eberth 2005; Ramezani et al. 2022; Fig. 2). It interfingers with and is overlain by Bearpaw Formation (BFm) marine shales. Eberth (2005) provided the most recent review of the formational stratigraphy and sedimentology at DPP. The paralic to nonmarine Foremost Formation (FFm) occurs in the subsurface at the Park and can only be examined by geophysical well logs and core. It consists of sandstones, mudstones, coals, and shales with local iron-rich concretions. The Oldman Formation (OFm) is a strictly alluvial unit but is partially exposed; only its uppermost 10–20 m is well exposed throughout the Park. It consists of poorly sorted sandstones and mudstones with local iron- and silica-rich concretions. The Dinosaur Park Formation (DPFm) is an alluvial, estuarine, paralic, and marine unit that is completely and well exposed throughout the Park (∼80 m). It consists of sandstones, mudstones, shales, carbonaceous shales, and coals with local iron-rich concretions. The lowest ∼25 m of the BFm is exposed at the Park and consists of laminated mudstone with localized ironstone and phosphatic concretions that variously contain fossils of ammonites and other marine-to-brackish invertebrates and vertebrates.

DPP is uniquely famous for its rich diversity and abundance of dinosaurs and other vertebrates (Eberth et al. 2001; Ryan and Russell 2001; Currie 2005; Eberth and Currie 2005; Henderson and Tanke 2010; Eberth and Evans 2011; Brown et al. 2013*a*, 2013*b*; Eberth 2017). More than 300 skulls and articulated, partial-to-complete skeletons of dinosaurs have been collected at DPP since 1912. More than 166 species of vertebrates are known from DPP, including at least 51 species of dinosaur (Eberth and Evans 2011; Brown et al. 2013*a*, 2013*b*; Eberth 2017). In a global context, DPP's dinosaur assemblage represents a significant percentage (∼7%) of known global dinosaur diversity for the entirety of the Mesozoic based on counts by Wang and Dodson (2006) and Benton (2008). The DPFm yields the vast majority of vertebrate fossils at the Park and, of those, approximately 80% are from the lower one-half (40 m) of the formation (Eberth and Currie 2005; Henderson and Tanke 2010; Eberth and Evans 2011; Brown et al. 2013*a*; Eberth 2017).

DPP's bentonites

Discrete beds of bentonite claystone are common in Upper Cretaceous strata of the WIB and throughout the stratigraphic section at DPP. Thomas et al. (1990) and Eberth et al. (1992) documented 15 discrete bentonite beds in the Oldman, Dinosaur Park, and Bearpaw formations at DPP, and since then a few additional bentonites have been noted. WIB bentonites represent diagenetically altered air-fall deposits of pyroclastic ash and tephra and have been commonly sampled for radioisotopic dating of their magmatic minerals (e.g., Goodwin and Deino 1989; Thomas et al. 1990; Obradovich 1993; Rogers et al. 1993; Lerbekmo 2002; Roberts et al. 2005; Foreman et al. 2008; Jinnah et al. 2009; Ramezani et al. 2022).

In outcrop, DPP's bentonites are easily recognized by their well-developed popcorn-textured surfaces—the result of clay expansion and shrinkage due to weathering. The Park's bentonites rarely can be traced for more than a few hundred meters in outcrop due to a combination of the natural limits of the alluvial/paralic facies that hosted the airfall deposits and a highly dissected/eroded modern badlands topography. Bentonite thicknesses range from a few mm up to ∼50 cm, and trenched exposures commonly reveal sharp upper and lower boundaries. Boundaries can also be diffuse or soft-sediment deformed, suggestive of deposition across a bioturbated (e.g., dinosaur-trampled) landscape or as the result of post-depositional bio- and phytoturbation. The claystone matrix is typically grey green but becomes a lighter color when dry (N9) and a darker color when moist or wet (5G 5/2, 5Y 6/4, 5Y 7/4). Whole rock samples typically yield silt-to-sand-sized volcanic phenocrysts (e.g., biotite, quartz, feldspar, and zircon) and organic fragments that exhibit normal grading through the deposit and are very often concentrated at or near the base of the deposit (e.g., Thomas et al. 1990). At some

Fig. 2. Belly River Group stratigraphy at Dinosaur Provincial Park based on outcrop and subsurface data as described by Eberth (2005). Magnetostratigraphy from Lerbekmo (2005). Gamma log is from the Princess Well (Alberta Research Council Core Hole 83-1). Composite outcrop section (right) was measured in the Iddesleigh area by DAE (23–24 July 1996; see Fig. 1). With the exception of BB and LCZB, which were observed in the measured section, bentonite placements are inferred using a variety of marker beds and surfaces shown here. Inset explains symbols and abbreviations used in the measured section. Bentonite abbreviations as in Fig. 1 and explained in the text. API, American Petroleum Institute units; BB, Bearpaw Bentonite; DPP, Dinosaur Provincial Park; Fe-stone, ironstone; Fm, Formation; FSB, Field Station Bentonite; JCB, Jackson Coulee Bentonite; LCZB, Lethbridge Coal Zone Bentonite; Lithostrat, Lithostratigraphy; Paleomag, Magnetostratigraphy; PT, Plateau Tuff.

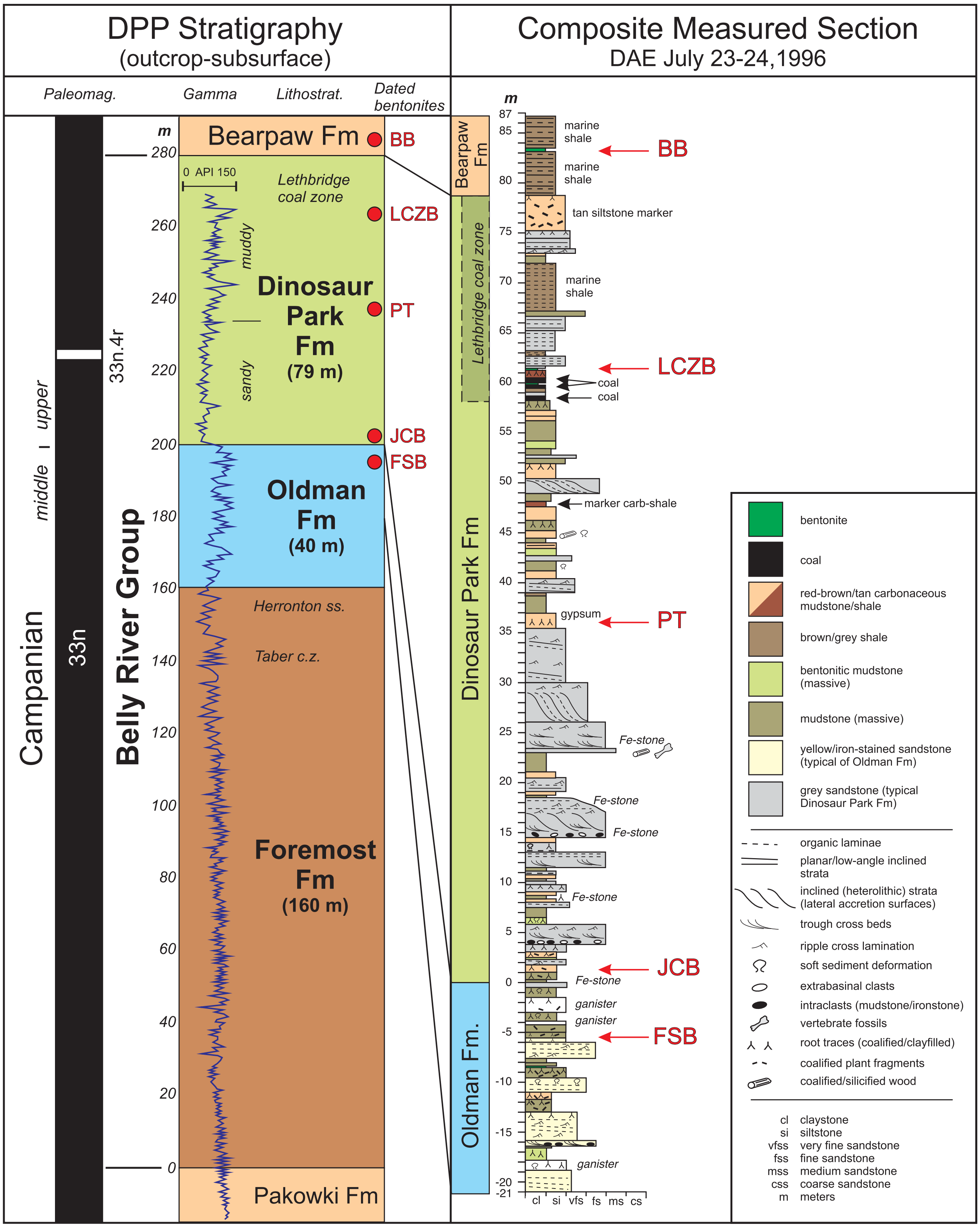

Can. J. Earth Sci. 00: 1–20 (2023) | dx.doi.org/10.1139/cjes-2023-0037

locations, phenocryst assemblages may comprise more than one normally graded succession, suggesting multiple pulses of airfall deposition and/or reworking (Thomas et al. 1990). Diagenetically precipitated gypsum crystals, limonite staining, coalified root traces, and plant fragments are common in these deposits (cf., Thomas et al. 1990), indicating a wide range of post-depositional physical and organic influences on the original airfall ash deposit over hours to years (Thomas et al. 1990; Eberth et al. 1992).

X-Ray diffraction analyses of the Plateau Tuff (PT)—the best-studied bentonite at DPP—indicate that the clay matrix is monomineralic, comprising pure smectite (Thomas et al. 1990). Similar results were reported by Rogers (1990), Rogers et al. (1993), and Foreman et al. (2008) for Campanian-age bentonites from the Two Medicine Formation of Montana. Based on the ubiquity of modern swelling behaviors, we assume a largely smectitic clay composition for all the bentonites discussed here. Thomas et al. (1990) showed the PT to be the result of devitrification of volcanic ash that was deposited as air-fall across a wetland landscape. Using x-ray fluorescence and electron microprobe analyses, they inferred that the tuff may have originated in the Elkhorn Mountain Volcanic complex of Montana. However, Foreman et al. (2008) have also shown that the Adel Mountain volcanics are a reasonable source for some of the younger and more mafic bentonites in the Two Medicine Formation, and thus, possibly, those in southern Alberta as well.

In ascending stratigraphic order, the five bentonites from DPP sampled and analyzed by Ramezani et al. (2022) and that are our focus are Field Station Bentonite (FSB), Jackson Coulee Bentonite (JCB), PT, Lethbridge Coal Zone Bentonite (LCZB), and Bearpaw Bentonite (BB). Each is briefly described below. The use of the term "Plateau Tuff" (instead of Plateau Bentonite) honors the widespread use of the term in the literature and is further validated by the presence of volcanic glass shards and "ghosted" pumiceous rock fragments in the matrix (Thomas et al. 1990).

Although each bentonite occurs in a different geographic location in the Park (Fig. 1) and cannot be traced continuously beyond a few hundred meters, their relative lithostratigraphic positions can be documented by reference to formational boundaries and other stratigraphic markers (Roberts et al. 2022). The stratigraphic section in which each bentonite is placed (Fig. 2) was measured in the Iddesleigh area of eastern-most DPP by DAE (23–24 July 1996). This area exposes the most complete, continuous, and accessible outcrop section in the Park. It includes all the formational boundaries and marker beds that are present elsewhere throughout the Park and encompasses the complete stratigraphic range of the bentonites described here and by Ramezani et al. (2022).

Field Station Bentonite

The FSB is 20 cm thick, occurs 5.5 m below the OFm–DPFm contact, and crops out in the area around the Royal Tyrrell Museum Field Station at DPP. Its placement in the Iddesleigh section (Fig. 2) is based on its stratigraphic occurrence relative to the OFm–DPFm contact near the Field Station building.

Jackson Coulee Bentonite

The JCB is a 50 cm thick, gritty bentonite dominated by silt-sized volcanic grains, pumice fragments, and a variety of as yet unidentified lithic fragments. It occurs 1.25 m above the OFm–DPFm contact and forms the lowest portion of a 2 m thick, deeply weathered bentonitic mudstone succession. It exhibits traces of laminae suggesting hydraulic reworking and differential settling, multiple eruptive pulses, or both. Its placement in the Iddesleigh section (Fig. 2) was determined by its occurrence relative to the OFm–DPFm contact at the mouth of Jackson Coulee, about 3 km southwest of the Iddesleigh section.

Plateau Tuff

The PT is 30 cm thick and occurs 36 m above the OFm–DPFm contact near the top of a stratigraphic succession exposed in the natural preserve (core) area of the Park (Thomas et al. 1990). It crops out locally along a prominent cliff-forming ridge referred to locally as the "Cathedral" (Wood 1989; Thomas et al. 1990). The PT is the most intensively studied bentonite in the Park and is interpreted as representing two or more short-duration accumulation events in an alluvial paludal/lacustrine (wetlands) setting (Thomas et al. 1990; Eberth et al. 1992). Its placement in the Iddesleigh section (Fig. 2) is based on its stratigraphic position relative to a carbonaceous shale marker bed (Figs. 2–4) that was traced in outcrop from the PT locality to the Iddesleigh area, a distance of ∼7 km. The shale is likely a precursor to sub-bituminous coals in the overlying Lethbridge Coal Zone and provides a reliable means of lithostratigraphic correlation in this area (Eberth 2005).

Lethbridge Coal Zone Bentonite

The LCZB is 13 cm thick and occurs within the lowest few meters of the Lethbridge Coal Zone, an approximately 15–20 m thick, organic-rich paralic zone at the top of the DPFm (Eberth and Hamblin 1993; Eberth 2005; Fig. 2) in the northeastern corner of the Park area, across the Red Deer River and ∼7 km northeast from the Iddesleigh section. There, it is hosted by an organic-rich mudstone succession that exhibits coalified roots and root traces. A correlative of the LCZB was recognized in the Iddesleigh section and was confirmed by comparing its position relative to the DPFm–BFm contact at both the LCZB locality and in the Iddesleigh section. In our measured section at Iddesleigh, the bentonite is placed 61.5 m above the OFm–DPFm contact and 17.25 m below the DPFm–BFm contact.

Bearpaw Bentonite

The BB is 30 cm thick, is hosted by drab-colored grey-brown marine shales, and occurs 4.5 m above the base of the BFm in the Iddesleigh section. In that area, the top of the DPFm is marked by a 2.5–3.5 m thick deposit of oxidized (red–brown tan) carbonaceous siltstone and shale that serves as a marker

Fig. 3. CA-ID-TIMS U–Pb geochronology of five bentonites at Dinosaur Provincial Park and the associated Bayesian age-stratigraphic model for the Park based on data from Ramezani et al. (2022). See the text for detailed discussion. Dashed curved lines define the 95% confidence interval error envelope of the model. Inset bar-plot shows an additional CA-ID-TIMS U–Pb zircon geochronology for the Plateau Tuff conducted by SLK at the Jack Satterly Geochronology Laboratory. Abbreviations as in Fig. 1. Additional abbreviations: BFm, Bearpaw Formation; BGC, Berkeley Geochronology Center; cm, centimeters; DPFm, Dinosaur Park Formation; JSGL, Jack Satterly Geochronology Laboratory; ka, kiloannum; Leth Coal Z, Lethbridge coal zone; Ma, Megaannum; m, meters; MSWD, mean square weighted deviation; n, number of grains analyzed; OFm, Oldman Formation.

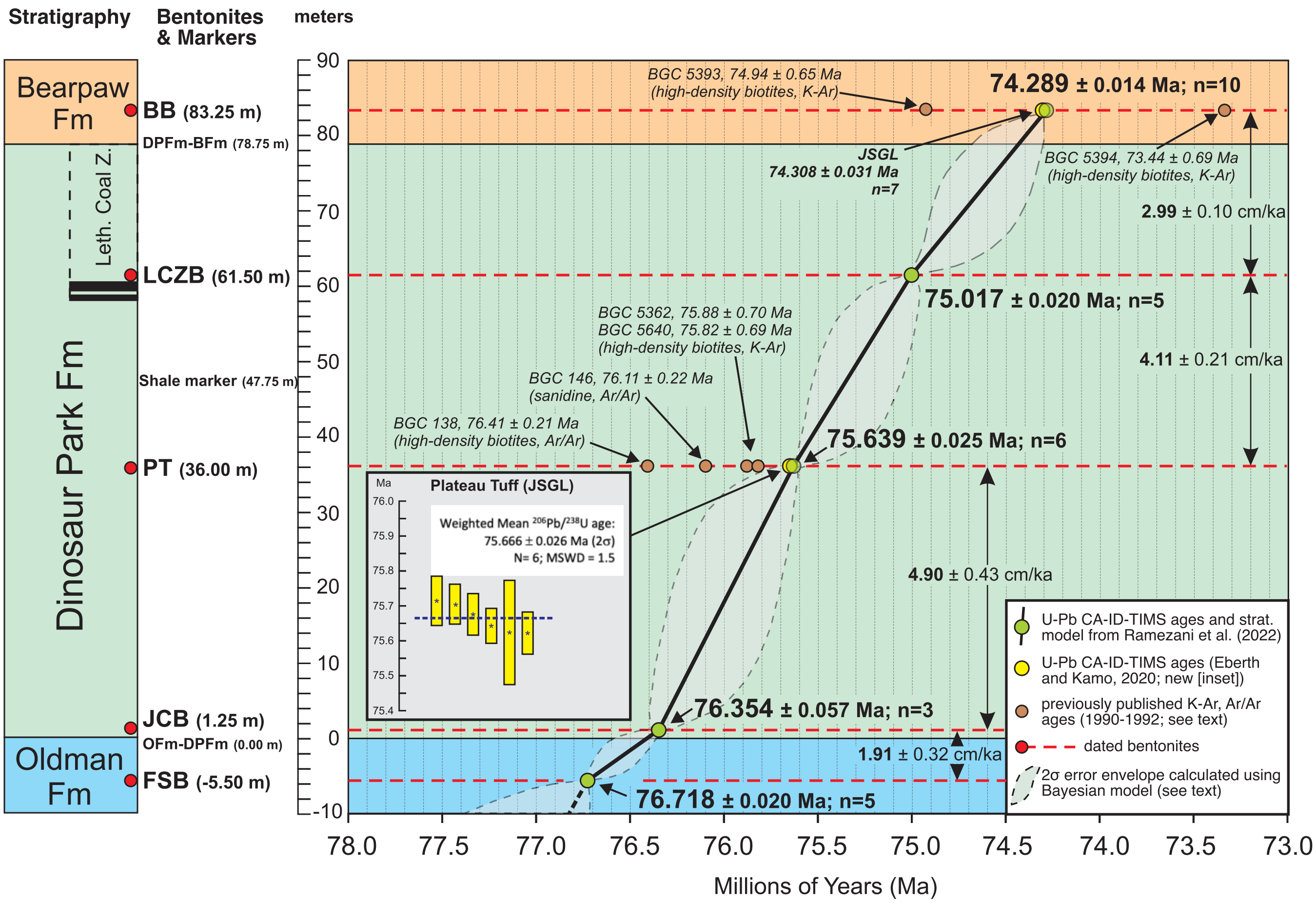

bed at the top of the nonmarine section and produces a nonmarine palynological assemblage (Fig. 2; Brinkman et al. 2005, fig. 26.1; Eberth 2005).

Brief history of radioisotopic geochronology at DPP

Prior to the recent U–Pb geochronology (Ramezani et al. 2022), three bentonites from DPP—the PT, BB, and the FSB—were dated using K–Ar and $^{40}Ar/^{39}Ar$ methods applied to hand-picked biotite, plagioclase, and sanidine phenocrysts (Thomas et al. 1990; Eberth and Deino 1992, 2005; Eberth et al. 1992; Eberth and Hamblin 1993; Eberth 2005), along with a number of other tuffs from correlative units across the WIB (compiled in Ramezani et al. 2022). From DPP, only results for the PT and BB were published with associated analytical data in peer-reviewed format (Thomas et al. 1990; Eberth et al. 1992; Fig. 3). Subsequently, Eberth and Hamblin (1993), Eberth and Deino (1992, 2005), and Eberth (2005) updated $^{40}Ar/^{39}Ar$ geochronology for bentonites from the Milk River Canyon area of southeastern-most Alberta. These formed the basis of a proposed age-stratigraphic model for the BRG in southern Alberta (Eberth and Hamblin 1993, fig. 19; Eberth 2005). However, these reports reflected geochronological work in progress without the necessary analytical details and thus remained preliminary. Subsequent attempts at $^{40}Ar/^{39}Ar$ geochronology of the BRG using the PT as a control produced inconsistent results due to technical matters (see below), preventing the preliminary ages from being finalized and properly reported.

As summarized by Ramezani et al. (2022), the legacy $^{40}Ar/^{39}Ar$ geochronology of the WIB during the late 1980s to the early 2000s reflected ongoing improvements in laboratory protocols and age-calculation parameters, including multiple revisions to the K decay constants and ages of mineral standards (e.g., Deino and Potts 1990; Renne et al. 1994, 1998, 2010, 2011; Min et al. 2001; Kuiper et al. 2008; Deino et al. 2010; Phillips and Matchan 2013). Predictably, the resulting inconsistencies combined with an overall piecemeal approach frustrated attempts to build a comprehensive,

Fig. 4. Radioisotopically calibrated litho- and biostratigraphy at Dinosaur Provincial Park (DPP) based on data presented here and our CA-ID-TIMS U–Pb age model for DPP (Table 3; Ramezani et al. 2022). Vertical axis is millions of years. Dotted lines indicating age boundaries between ammonite biozones are placed following Ogg and Hinnov (2012) and Gale et al. (2020). Palynomorph biozones from Braman (2013, 2018). Dinosaur assemblage zones from Eberth and Getty (2005), Ryan and Evans (2005), Evans (2007), Evans et al. (2009), Mallon et al. (2012) and Brown (2014). All abbreviations as in Figs. 2 and 3.

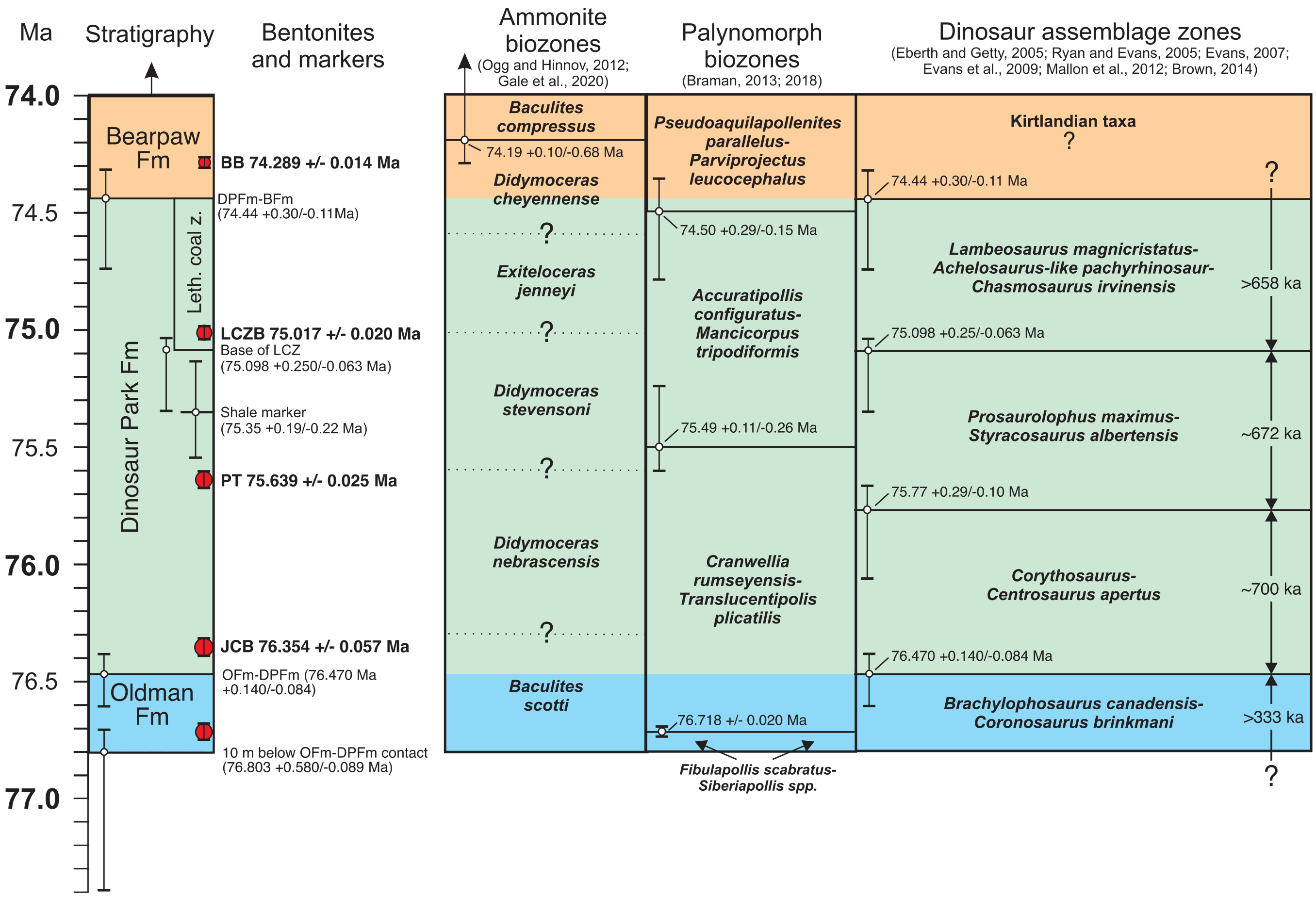

high-resolution, reproducible geochronology for the Park and the BRG, as well as correlation to other Campanian-age dinosaur sites with $^{40}Ar/^{39}Ar$ ages in the WIB (e.g., Goodwin and Deino 1989; Rogers et al. 1993; Ogg et al. 2004; Roberts et al. 2005, 2013; Foreman et al. 2008; Jinnah et al. 2009).

A road map for systematic U–Pb zircon geochronology of bentonites from Campanian-age dinosaur localities of the Western Interior, envisioned by the late Sam Bowring at the Massachusetts Institute of Technology (MIT) and Eric Roberts at James Cook University, took shape by 2012. The approach was unique in that its goals were to collect key bentonites from target units in New Mexico, Utah, Montana, and Alberta and to produce a set of internally consistent U–Pb age data employing the latest community-wide analytical practices and protocols for the CA-ID-TIMS method. It would thereby create a basin-wide, high-resolution, chronostratigraphic framework (baseline) upon which meaningful biostratigraphic correlations and dinosaur paleobiological interpretations could be based. The outcomes of the decade-long effort now serve as a foundational geochronological study of Campanian dinosaurs in the WIB (Ramezani et al. 2022). The study reported ages from the five DPP bentonites described above, which together supersede all previously published ages for the DPP section. In ascending order, the ages (with 2σ analytical errors) are FSB, 76.718 ± 0.020 Ma; JCB, 76.354 ± 0.057 Ma; PT, 75.639 ± 0.025 Ma; LCZB, 75.017 ± 0.020 Ma; and BB, 74.289 ± 0.014 Ma (Table 1).

A comparable effort in establishing a U–Pb CA-ID-TIMS geochronology for the Campanian–Maastrichtian age Horseshoe Canyon Formation (HCFm) of south-central Alberta at the Jack Satterly Geochronology Laboratory (JSGL) of the University of Toronto (Eberth and Kamo 2020) provided an independent age for the BB (74.308 ± 0.031 Ma) that serves as a test point for interlaboratory comparison and accuracy assurance (see Ramezani et al. 2022). A second test reported here is a CA-ID-TIMS U–Pb zircon age for a duplicate sample of the PT analyzed at JSGL in 2019. The consistency of the two bentonite ages reported by MIT and JSGL provides a quantitative test of reproducibility of the CA-ID-TIMS U–Pb method as applied to the BRG. Figure 3 illustrates the U–Pb-based age-stratigraphic (Bayesian) model for the DPP, including the previously published $^{40}Ar/^{39}Ar$ results from the PT (Thomas et al. 1990; Eberth et al. 1992), without any re-

Canadian Science Publishing

Table 1. U–Pb isotopic data for zircon from the Plateau Tuff, Dinosaur Provincial Park, Alberta (Jack Satterly Geochronology Laboratory, University of Toronto).

Sample fractions*	Pb_c† (pg)	Pb‡*/Pb_c†	U† (pg)	Th/U§	Ratios								Ages (Ma)						
					$^{206}Pb/^{204}Pb$‖	$^{208}Pb/^{206}Pb$¶	$^{206}Pb/^{238}U$#	Err(2σ%)	$^{207}Pb/^{235}U$#	Err(2σ%)	$^{207}Pb/^{206}Pb$#	Err(2σ%)	$^{206}Pb/^{238}U$	Err(2σ)	^{207}Pb	Err	^{207}Pb	Err	Corr.
Plateau Tuff																			
Z1	1.5	21.6	2772	0.43	1388.5	0.138	0.011814	0.094	0.07617	1.42	0.04678	1.40	**75.714**	**0.071**	74.54	1.02	37	34	0.142
Z2	2.1	12.2	2139	0.50	774.4	0.158	0.011813	0.074	0.07757	0.93	0.04765	0.96	**75.705**	**0.056**	75.86	0.70	81	23	0.065
Z3	1.9	9.9	1557	0.44	643.3	0.140	0.011808	0.078	0.07773	0.96	0.04776	0.69	**75.676**	**0.059**	76.01	0.50	86	16	0.010
Z4	0.6	20.5	999	0.52	1279.0	0.164	0.011803	0.066	0.07742	0.49	0.04759	0.48	**75.642**	**0.050**	75.71	0.36	78	11	0.136
Z5	1.6	8.2	1099	0.46	533.7	0.146	0.011800	0.196	0.07736	1.73	0.04757	1.70	**75.623**	**0.149**	75.66	1.26	77	40	0.210
Z6	1.6	16.8	2181	0.45	1072.2	0.144	0.011800	0.078	0.07621	1.20	0.04686	1.29	**75.621**	**0.060**	74.58	0.93	41	31	0.039
													75.666 ± 0.026 Ma; MSWD = 1.5						

Note: Corr. coef., correlation coefficient. Ages calculated using the decay constants $\lambda_{238} = 1.55125E\text{-}10\ year^{-1}$ and $\lambda_{235} = 9.8485E\text{-}10\ year^{-1}$ (Jaffey et al. 1971).
*All analyses are single zircon grains and pre-treated by the thermal annealing and acid leaching (CA-TIMS) technique. Data used in date calculation are in bold.
†Pb(c) is total common-Pb in analysis. Pb‡ is radiogenic Pb concentration. Total sample U content in pg.
§Th content is calculated from radiogenic ^{208}Pb assuming concordance between U–Pb and Th–U systems.
‖Measured ratio corrected for spike and fractionation only.
¶Radiogenic Pb ratio.
#Corrected for fractionation, spike, and blank. Also corrected for initial Th/U disequilibrium using radiogenic ^{208}Pb and $Th/U_{[magma]} = 2.8$.
Mass fractionation based on $^{202}Pb/^{205}Pb$ ratio of tracer (~0.18% ± 0.04%/amu) was applied to single-collector Daly analyses.
All common Pb assumed to be laboratory blank. Total procedural blank less than 0.1 pg for U.
Blank isotopic composition: $^{206}Pb/^{204}Pb = 18.20 \pm 0.45$, $^{207}Pb/^{204}Pb = 15.29 \pm 0.24$, $^{208}Pb/^{204}Pb = 37.16 \pm 0.77$. MSWD, mean square weighted deviation.

calculation of the legacy data or incorporation of systematic uncertainties.

Methods

The bentonite U–Pb geochronology and the Bayesian age-stratigraphic model employed here for the Dinosaur Park outcrop section are reproduced from Ramezani et al. (2022) and are also discussed in Beveridge et al. (2022). Also included are the independently determined U–Pb zircon ages of the BB from Eberth and Kamo (2020) and of the PT reported here (Table 1) for assessing reproducibility. Those publications describe the details of CA-ID-TIMS analytical procedures, age calculation methodology, and age-stratigraphic modelling. Figure 3 illustrates the age model for the Dinosaur Park section with its 95% confidence interval error envelope.

Six single zircon U–Pb analyses by the CA-ID-TIMS method from the PT carried out at JSGL produced a weighted mean $^{206}Pb/^{238}U$ date of $75.666 \pm 0.026/0.033/0.087$ Ma (mean square weighted deviation (MSWD) = 1.5) without any outliers (Table 1, Fig. 3), using chiefly the same analytical procedures as those described in Eberth and Kamo (2020). The only exceptions are the natural U isotopic composition of 137.818 ± 0.044 (Hiess et al. 2012) and an initial magma Th/U ratio of 2.8 ± 1.0 used for data reduction here for the sake of consistency with those of Ramezani et al. (2022). Because both MIT and JSGL use the same EARTHTIME mixed U–Pb tracer solution for ID-TIMS analysis, their systematic age uncertainties can be ignored in comparing their results.

The DPP age-stratigraphic model of Ramezani et al. (2022) used five U–Pb tuff ages combined with their precise stratigraphic positions and the Bayesian statistics of the Bchron software (Haslett and Parnell 2008; Parnell et al. 2008) to extrapolate stratigraphic ages with objective (asymmetrical) uncertainties without the assumption of constant rock accumulation rates. All lithostratigraphic and biozonal boundary ages and error presented here are extrapolated from the above model (Fig. 3).

Reproducibility of CA-ID-TIMS U–Pb ages

Eberth and Kamo (2020) reported an age of 74.308 ± 0.031 Ma for the BB in their study of the chronostratigraphy of the dinosaur-rich Campanian–Maastrichtian age HCFm of south-central Alberta. As indicated by Ramezani et al. (2022), the weighted mean $^{206}Pb/^{238}U$ dates for the BB reported by the two laboratories (Fig. 3) fall within the reported 2σ ranges of their analytical uncertainties, with the age reported by Eberth and Kamo (2020) being 0.26‰ older. Ramezani et al. (2022) also pointed out that this difference could be reduced to 0.16‰ by using similar data reduction values corresponding to the natural U isotopic composition and the initial magma Th/U ratio. The new U–Pb zircon age for the PT (75.666 ± 0.026 Ma) is 0.36‰ older than the age of 75.639 ± 0.025 Ma for the PT reported by Ramezani et al. (2022), still well within the reported 2σ uncertainties of the weighted mean age (Fig. 3).

The strong overlap of the weighted mean ages for the BB and PT from different laboratories underscores the accuracy and reproducibility of the modern U–Pb CA-ID-TIMS geochronological method. In turn, reproducibility indicates that U–Pb ages can be compiled over time to build a larger age data set for the Park's strata and fossils and to provide increasingly finer chronostratigraphic resolution for BRG and correlative stratigraphic sections at the Park and elsewhere. In the following sections, we use the results of Ramezani et al. (2022) to calibrate rock accumulation rates and biostratigraphic zonations at DPP.

Rock accumulation rates

The 88.75 m stratigraphic section that extends from the FSB (5.5 m below the OFm–DPFm contact) to the BB (4.5 m above the DPFm–BFm contact) encompasses ∼2.43 Myr, with an overall rock accumulation rate of 3.65 ± 0.04 cm/ka (Table 2). However, with five U–Pb ages available to us that encompass almost the complete exposed section at the Park, we can calculate and compare average rock accumulation rates for different intervals in the section, including the uppermost OFm and lower, middle, and upper portions of the DPFm (Table 2; Fig. 3). In ascending order, these are 1.91 ± 0.32, 4.90 ± 0.43, 4.11 ± 0.21, and 2.99 ± 0.10 cm/ka, respectively. Each is indicated by a separate segment/slope along the age-stratigraphy line and is reported with 2σ error from the Bayesian age model (Table 2).

Two aspects of the age-stratigraphy line are of interest. First, there is a strong inflection that highlights both an unusually low rock accumulation rate (1.91 ± 0.32 cm/ka) in the uppermost portion of the OFm and an overall increased rock accumulation rate for the entire DPFm. Secondly, the line shows a steady decrease in rock accumulation rates upward through the DPFm. We discuss these patterns and their significance below.

The low rock accumulation rate in the uppermost OFm

A rate of 1.91 ± 0.32 cm/ka for the uppermost OFm is unusually low for alluvial units in the distal foredeep of the Alberta Basin (cf., Lerbekmo 1989; Eberth and Hamblin 1993; Lerbekmo 2005; Eberth and Braman 2012; Eberth and Kamo 2020). Where present, such values are typical of intervals where unconformities and/or hiatus(es) are present (e.g., the Whitemud-Battle-Scollard succession; Russell 1983; Eberth and Braman 2012; Eberth and Kamo 2019). Braman and Koppelhus (2005; fig. 6.4) described a stratigraphically coincident first occurrence of six nonmarine palynomorph taxa at the "very top" of the OFm at DPP, about three meters or so below the discontinuity but no lower than the FSB and not 10 m below the discontinuity as illustrated in their fig. 6.4 (DRB, personal communication, 2016). Subsequent study of this assemblage (Braman 2013, 2018, pp. 29–31) resulted in it being amended to five taxa and being designated as the *Cranwellia rumseyensis–Translucentipolis plicatilis* palynological biozone, ranging from the uppermost OFm (∼FSB) to ∼42 m above the base of the DPFm at DPP (Fig. 4). Although first occurrences of the biozone's defining taxa are stratigraphically coincident at or slightly above the FSB in the OFm, first appear-

Table 2. Rock accumulation rates at Dinosaur Provincial Park.

			Data							Rates			
Stratigraphic interval	Sample	Tuff name	Height (m)	*T* (Ma)	±(2σ)	Δ*T* (ka)	±	Δ*h*	Min	Max	cm/ka	±
	IL082717-1	Bearpaw	83.25	74.289	0.014							
LCZ–Bearpaw						728	24	21.75	2.89	3.09	**2.99**	0.10
	LCZ2	LCZ	61.5	75.017	0.020							
Plateau–LCZ						622	32	25.50	3.90	4.32	**4.11**	0.21
	CD082717-1	Plateau	36	75.639	0.025							
JC–Plateau						715	62	34.75	4.47	5.32	**4.90**	0.43
	JC082817-1	JC	1.25	76.354	0.057							
Field Station–JC						364	60	6.75	1.59	2.22	**1.91**	0.32
	FS082717-1	Field Station	−5.5	76.718	0.020							
Dinosaur Park Fm (JC–BB)						2065	59	82.00	3.86	4.09	**3.97**	0.11
Complete section (FSB–BB)						2429	24	88.75	3.62	3.69	**3.65**	0.04

Note: LCZ, Lethbridge Coal Zone; JC, Jackson Coulee; BB, Bearpaw Bentonite; **FSB,** Field Station Bentonite.

ances of these same taxa are staggered through a 10 m stratigraphic interval in exposures of the OFm in the Milk River canyon area of southeastern Alberta (Braman 2018). Additionally, in that region, the biozone terminates approximately 40 m higher in the OFm and fails to reach into the DPFm, the base of which occurs in a stratigraphically higher position compared to DPP (Eberth and Hamblin 1993; Eberth in press).

This complex stratigraphic and paleogeographic distribution pattern of palynomorphs in the *C. rumseyensis*–*T. plicatilis* palynological biozone from DPP to the Milk River area suggests that the uppermost OFm section at DPP likely contains a temporally condensed interval or hiatus relative to time-equivalent strata in the Milk River area of southeastern Alberta and thus may help explain the unusually low rock accumulation rate in the uppermost OFm exposed at DPP. Assuming that the rock accumulation rate for an uncondensed section of the OFm at DPP would likely not exceed that of the immediately overlying DPFm (4.90 ± 0.43 cm/ka), which was deposited during an episode of increased sediment supply (Eberth and Hamblin 1993; Eberth in press) and increased accommodation (Rogers et al. 2023), we estimate that the condensed section/hiatus between the FSB and the JCB cannot represent more than ∼227 ka.

Increased rock accumulation rate in the DPFm versus the OFm

The DPFm shows an overall rock accumulation rate of 3.97 ± 0.11 cm/ka (Table 2). This value is twice that observed for the top of the OFm (1.91 ± 0.32 cm/ka) and conforms to an interpretation of increased rock accumulation rate associated with accommodation during the onset of the Bearpaw transgression across the Judith River–Belly River wedge (e.g., Eberth 2005; Rogers et al. 2016, 2023). It also conforms to the interpretation of Eberth and Hamblin (1993), who proposed that regionalized cordilleran tectonics and unroofing of the proximal foredeep resulted in a sharp increase in sediment supply upward across the OFm–DPFm discontinuity and expansion of the Dinosaur Park clastic wedge to the southeast during the Bearpaw transgression.

The difference in the amount of overall rock accumulation rates between the DPFm at DPP (∼4.0 cm/ka) versus the Coal Ridge Member in north-central Montana (∼8.7 cm/ka)—the two units whose bases are interpreted as marking the isochronous onset of the Bearpaw transgression at ∼76.3 Ma across the Judith River–Belly River wedge (Rogers et al. 2023)—is likely due to their proximal–distal locations relative to the foredeep, with the Montana section occupying a more distal position in the basin relative to DPP. These different relative positions are confirmed by the significantly older age of the base of the BFm in the Montana section (∼75.2 Ma) versus the much younger age of the base of the BFm at DPP (∼74.4 Ma) (Ramezani et al. 2022; Rogers et al. 2023).

Decreasing rock accumulation rates upward through the DPFm

Upward through the DPFm (Table 2, Fig. 3), rock accumulation rates decline from 4.90 ± 0.43 cm/ka in the lower 36 m of the formation to 4.11 ± 0.21 cm/ka in the middle of the formation and to 2.99 ± 0.10 cm/ka in the uppermost 17.25 m of the formation (the Lethbridge Coal Zone) and lowermost 4.5 m of the BFm. During a steady rate of sediment supply, a decline in rock accumulation rates is unexpected under conditions of increasing accommodation and expansion of marine settings that result from a eustatic rise in sea level (documented for this time interval (Kauffman and Caldwell 1993; fig. 5 in Ramezani et al. 2022)). A reduction in rock accumulation rates at DPP during the Bearpaw transgression can be explained, however, if one considers the evidence for declining sediment supply rates in the DPFm during a time of eustatic (global) sea-level rise. In its lower 30–40 m, the DPFm is overwhelmingly dominated by paleochannel sandstones (sandstone/mudstone ratios > 1) and frequent occurrences of stacked paleochannel successions that are more than 20 m in thickness (Eberth and Hamblin 1993; Hamblin 1997; Eberth 2005). This indicates that, initially, sediment supply was higher than could be accommodated fully and that paleochannel stacking and some degree of sediment bypassing resulted in the preferred preservation of channel

 Can. J. Earth Sci. **00:** 1–20 (2023) | dx.doi.org/10.1139/cjes-2023-0037

sandstones (and dinosaur fossils) in the stratigraphic pile (cf., Legarreta and Uliana 1998; Blum and Tornquist 2000). Upward through the DPFm, however, a declining depositional slope, declining rates of flow, and overall declining sediment supply are suggested by a combination of features including (1) the disappearance of extraformational cobbles in channel lag deposits, (2) declining grain sizes in coarse-grained facies, (3) the appearance and preservation of widespread coal and carbonaceous shales in the upper 40 m of the section, (4) decreasing dimensions of paleochannels, and (5) declining occurrences of fully preserved megaherbivore and large theropod dinosaur skeletons (Wood 1989; Eberth and Hamblin 1993; Hamblin 1997; Eberth 2005; Eberth and Currie 2005). Accordingly, although eustatic (global) sea-level rise continued during deposition of the DPFm, a reduction in sediment supply rates—likely caused by changing upstream tectonic influences on depositional slope and possibly climatic conditions (Eberth and Hamblin 1993)—resulted in an overall decline in rock accumulation rates after an initially large pulse of sediment supply. Similarly complex patterns in parts of the western Canada Foreland Basin are described by Catuneanu and Sweet (1999), Eberth and Braman (2012), Eberth and Kamo (2019), and Eberth (in press), highlighting the relative influence of eustasy, climate, and tectonics on stratigraphic evolution and architecture in foreland basins and other nonmarine settings (cf., Shanley and McCabe 1998; Blum and Tornquist 2000).

Calibrated palynostratigraphic biozones

Braman (2018) provided the first palynological biozonation scheme for the Alberta Basin. It ranged in age from the Santonian to lower Paleocene and referred to preliminary $^{40}Ar/^{39}Ar$ geochronologic data summarized in Eberth (2005) to calibrate some of the zones. Here, we update those calibrations as they relate to the Park using the data of Ramezani et al. (2022). Braman (2018) recognized portions or all of four palynological biozones at the Park (Fig. 4). These are described and calibrated here in ascending stratigraphic order. A small portion of the *Fibulapollis scabratus–Siberiapollis* spp. biozone is present at the base of the exposed section below the FSB. Based on its relationship to the FSB, we regard it as older than 76.718 Ma but cannot assess its maximum age. The *Cranwellia rumseyensis–Translucentipollis plicatilis* biozone overlies the latter, ranges in age from 76.718 ± 0.20 to $75.49 + 0.11/-0.26$ Ma extending up into the middle of the DPFm (between the PT and the marker shale), at an inferred stratigraphic position of ∼42 m above the OFm–DPFm contact. As discussed above, it provides evidence for a condensed section or hiatus at DPP relative to the temporally equivalent but more complete section in the OFm of the Milk River drainage area of southeastern Alberta (Braman 2018). The *Accuratipollis configuratus–Mancicorpus tripodiformis* biozone extends up section from above the PT to just below the BFm (Braman 2018) and ranges in age from $75.49 + 0.11/-0.26$ to $74.50 + 0.29/-0.15$ Ma. Lastly, the *Pseudoaquilapollenites parallelus–Parviprojectus leucocephalus* biozone is partially preserved at DPP predominantly at the base of the BFm but may extend up to the Dorothy Bentonite of the BFm near Drumheller (Eberth and Kamo 2020). It thus ranges in age from $74.50 + 0.29/-0.15$ to ∼73.7 Ma.

Geochronological calibration of Braman's palynological biozones in Edmonton Group strata of south-central Alberta have provided an additional means of correlating late Maastrichtian strata from the Hell Creek Formation of northeastern Montana to the Scollard Formation of southern Alberta (Eberth and Kamo 2019, 2020). We anticipate that our geochronological calibration of the Park's palynological biozones may similarly assist with correlating southern Alberta's Campanian-age strata into northern and southern regions of western Alberta, farther north into Alaska (Prince Creek Formation), and south through the Milk River region into Montana (Judith River and Two Medicine formations).

Calibrated ammonite biozones

The well-established ammonite biostratigraphy of the WIB, along with an extensive data set of $^{40}Ar/^{39}Ar$ bentonite ages, has been used to construct a North American standardized Late Cretaceous time scale (Cobban et al. 2006; Ogg and Hinnov 2012; Gale et al. 2020). These $^{40}Ar/^{39}Ar$ ages were based on legacy multi-grain sanidine analyses at the USGS lab (Obradovich 1993), with limited reproducibility by modern standards (see above). The CA-ID-TIMS U–Pb geochronology and age-stratigraphy model employed here can be used to test the existing calibration of the Campanian-age ammonite biozones.

Tsujita (1995) proposed that the base of the BFm in southern Alberta could be assigned consistently to the *Baculites compressus* ammonite biozone. Specimens of *B. compressus* collected from ∼10 m above the base of the BFm at DPP (above the BB) broadly confirm this interpretation (e.g., Royal Tyrrell Museum of Palaeontology specimens: TMP1973.008.0406 and TMP1973.008.0447) and can be assigned an age of $74.19 + 0.10/-0.68$ Ma by extrapolating from our age model. Eberth et al. (1990) used palynological evidence, marine biostratigraphic data from western Saskatchewan, and radioisotopic data from Thomas et al. (1990) to suggest that the OFm–DPFm contact at DPP occurs within the *Baculites scotti* biozone (and that the *B. compressus* biozone occurs at or near the top of the exposed section). Again, extrapolating from our age-stratigraphy model (Fig. 3), this latter interpretation suggests that the *B. scotti* biozone should encompass the $76.47 + 0.14/-0.08$ Ma age of the OFm–DPFm contact. Our two extrapolated ages of 74.19 and 76.47 Ma for stratigraphic occurrences within the *B. compressus* and *B. scotti* biozones, respectively, fall within Gale et al.'s (2020) age ranges for these two biozones (74.2–73.9 Ma for *B. compressus* and 76.9–76.3 Ma for *B. scotti*). Accordingly, we tentatively accept the age ranges of the four-intervening ammonite biozones reported in Ogg and Hinnov (2012) and updated in Gale et al. (2020) (Fig. 4). In the geochronological context of ammonite zonations, the exposed section at DPP spans parts or all of six ammonite biozones, each with durations of ∼0.7–0.4 Myr (Fig. 4).

Calibrated dinosaur assemblage zones

Dinosaurian megaherbivore species, specifically hadrosaurs and ceratopsians, are stratigraphically partitioned in the Belly River and Edmonton groups of southern Alberta (Holmes et al. 2001; Currie and Russell 2005; Eberth and Getty 2005; Ryan and Evans 2005; Ryan and Russell 2005; Evans 2007; Evans and Reisz 2007; Evans et al. 2009; Eberth et al. 2010; Mallon et al. 2012; Eberth et al. 2013*a*; Evans et al. 2013, 2014; Eberth and Kamo 2020; Eberth in press). These differential distributions were consistent enough to be recognised by the early collectors (Sternberg 1950) and subsequently allowed for the recognition of informal dinosaur assemblage zones at DPP (e.g., Ryan and Evans 2005; Mallon et al. 2012; Eberth et al. 2013*a*; Evans et al. 2014).

One of the most notable changes in dinosaur assemblages at the Park occurs across the OFm–DPFm contact. Although the record of dinosaurs from the OFm at the Park is limited, none of the three large-bodied species recovered from the formation—the hadrosaurine *Brachylophosaurus canadensis*, the centrosaurine *Coronosaurus brinkmani*, and the tyrannosaurine *Daspletosaurus torosus* (but also see Carr et al. 2017)—are known to occur in the overlying DPFm, an interval that has been intensely sampled and studied for more than 100 years (Currie 2005; Currie and Russell 2005). Conversely, whereas chasmosaurine ceratopsids and lambeosaurine hadrosaurids are abundant in the DPFm, there is no evidence for them in the underlying OFm at DPP or elsewhere in southern Alberta. Furthermore, there is evidence for at least three dinosaur assemblage zones in the DPFm that can be defined by occurrences of 2–3 megaherbivore taxa. The stratigraphic succession of four assemblage zones at DPP may represent evolutionary changes within lineages of hadrosaurids and ceratopsids and/or ecological replacement of taxa in response to differential habitat preferences related to proximity to shoreline and/or latitudinal climate gradients (Sternberg 1950; Béland and Russell 1978; Brinkman 1990; Baszio 1997*a*, 1997*b*; Brinkman et al. 1998; Holmes et al. 2001; Currie and Russell 2005; Eberth and Getty 2005; Ryan and Evans 2005; Ryan and Russell 2005; Evans 2007; Evans et al. 2009; Mallon et al. 2012; Evans et al. 2013, 2014; Brown et al. 2020; Lowi-Merri and Evans 2020; Eberth in press).

The dinosaur assemblage zones described here remain informal and are based on a combination of first- and last-known stratigraphic occurrences for some of the well-represented megaherbivores known from DPP (typically represented by 10 or more specimens; see Supplementary data in Currie and Koppelhus 2005), as well as occurrences of poorly represented megaherbivore taxa within those ranges or within limited lithostratigraphic intervals at the top or bottom of the exposed section (e.g., OFm and Lethbridge Coal Zone). The reader is directed specifically to Supplementary sections in Currie and Koppelhus (2005) and Mallon et al. (2012) for access to specimen data sets with which to assess the numbers of individuals for each taxon and thus the robustness of taxonomic data sets.

Because some of the Park's megaherbivore taxa are recognized elsewhere in Alberta and Montana, they suggest an emerging potential for the Park's dinosaur assemblage zones to be elevated to formal biozones and biochrons in the northern portion of the WIB (e.g., Fowler 2017). However, such an undertaking requires larger sample sizes for some of the taxa, detailed documentation of their occurrences, and verification of their chronostratigraphic equivalency by independent radioisotope geochronology at locations beyond the limits of DPP. That said, we remain optimistic that ongoing paleontological and geological work being conducted in western Saskatchewan, along the Milk River drainage of southern Alberta, across northern and central Montana will eventually allow for such formalization. Below, we describe and calibrate the four informal dinosaurian assemblage zones at DPP (Fig. 4). We also review occurrences of some of the taxa in locations beyond DPP as a step toward establishing dinosaur biozones and biochrons in the future.

Brachylophosaurus–Coronosaurus assemblage zone (76.47 – 76.80+ Ma)

Although we can reliably place the upper boundary of this zone at the OFm–DPFm contact (76.470 + 0.14/−0.084 Ma; Fig. 3), there are no data currently available with which to confidently assign a lower age boundary for the assemblage; age projections at 10 or more meters below the contact and beyond the lowest dated bentonite (FSB) become associated with such large model-age errors that analysis is pointless (e.g., 76.803 + 0.58/−0.089 Ma; Table 3, Fig. 3). That said, we anticipate that new chronostratigraphic data from the Milk River canyon region of southeastern Alberta (Federico Fanti, personal communication, 2023) should be able to clarify the age range of this assemblage zone.

Exposures of the OFm at DPP yield the hadrosaurine *Brachylophosaurus canadensis* and the centrosaurine *Coronosaurus brinkmani*, two genera that are notably absent from the overlying, fossil-rich DPFm. The genus *Brachylophosaurus* is represented at DPP by two specimens, including the holotype, which was collected 7.5 m below the OFm–DPFm contact (Cuthbertson and Holmes 2010). The taxon is well represented regionally, including farther south in the Milk River, Judith River, and Malta areas of Alberta and Montana (Weishampel et al. 2004; Prieto-Marquez 2005, 2007; Tweet et al. 2008; Cuthbertson and Holmes 2010; Freedman-Fowler and Horner 2015).

The centrosaurine genus *Coronosaurus* (Ryan et al. 2012) is known from two and possibly a third monodominant bonebed assemblage that occurs more than 10 m below the OFm–DPFm discontinuity at DPP. The taxon is also known from a bonebed in the OFm along the Milk River Ridge in southern Alberta, which has been suggested to be penecontemporaneous with its range at DPP (Ryan and Russell 2005).

The ankylosaurid *Scolosaurus cutleri* (Penkalski and Blows 2013) may be characteristic for this level as well (Arbour and Currie 2013). Sternberg (1950) placed a quarry stake (Q080) in the lower part of the DPF, but other evidence suggests the quarry was in the OFm (Arbour and Currie 2013). Numerous specimens of this taxon have been recovered from the Two Medicine Formation of Montana (Arbour and Currie 2013), although there is some dispute as to whether or not the Montana specimens represent a different taxon (Penkalski 2013).

Table 3. Extrapolated ages of litho- and biostratigraphic picks from Bayesian age model at Dinosaur Provincial Park.

Picks	Above/below OFm–DPFm contact (m)	Measured/inferred age (Ma)	2σ error (Myr)	
			+	−
Baculites compressus specimens	88.75	74.19	0.10	0.68
BB*	83.25	74.289	0.014	0.014
DPFm–BFm boundary	78.75	74.44	0.30	0.11
Accuratipollis–Parviprojectus boundary	∼77	74.50	0.29	0.15
LCZB*	61.50	75.017	0.020	0.020
Base of LCZ	58.25	75.098	0.25	0.063
Shale marker	47.75	75.35	0.19	0.22
Cranwellia–Accuratipollis boundary	∼42	75.49	0.11	0.26
PT*	36.00	75.639	0.025	0.025
Corythosaurus–Styracosaurus boundary	∼30	75.77	0.29	0.10
JCB*	1.25	76.354	0.057	0.057
OFm–DPFm	0.00	76.470	0.14	0.084
FSB*	−5.50	76.718	0.020	0.020
Base of measured section	−10.00	76.803	0.58	0.089

*Measured U–Pb age of bentonite bed. Data from Ramezani et al. (2022). OFm, Oldman Formation; DPFm, Dinosaur Park Formation; BB, Bearpaw Bentonite; BFm, Bearpaw Formation; LCZB, Lethbridge Coal Zone Bentonite; PT, Plateau Tuff; JCB, Jackson Coulee Bentonite; FSB, Field Station Bentonite.

The tyrannosaurid *Daspletosaurus torosus*, also known from the upper part of this zone, is absent from the overlying DPFm at DPP, although the genus persists with what appears to be a distinct species (Currie 2003). Another specimen of *D. torosus* is known from the lower part of the DPFm along the Milk River, but the OFm–DPFm contact is time transgressive (Eberth and Hamblin 1993) and the site likely represents an equivalent time to the DPP specimen (Federico Fanti, personal communication, 2023; cf., Chiba et al. 2015). The genus has broad geographical range (Alberta and Montana) and might also have a broad chronostratigraphic range based on its occurrence in the Oldman, Dinosaur Park, Judith River, and Two Medicine formations (Currie 2005; Carr et al. 2017; Warshaw and Fowler 2022). For now, the species-level taxonomy of *Daspletosaurus* is in flux and unsuitable as an index taxon.

Corythosaurus–Centrosaurus assemblage zone (76.47–75.77 Ma)

This assemblage zone ranges in age from 76.470 + 0.14/−0.084 Ma at the OFm–DPFm contact to 75.77 + 0.29/−0.10 Ma at the top of the zone placed at ∼30 m above the contact (Ryan and Evans 2005; Table 3, Fig. 3). It has a duration of approximately 700 ka. The lower 30 m of the DPFm is characterized by the presence of the lambeosaurines *Corythosaurus* (consisting of two stratigraphically successive species, *Corythosaurus casuarius* and *Corythosaurus intermedius*) and *Parasaurolophus walker* (Evans et al. 2009), the hadrosaurine *Gryposaurus notabilis* (Lowi-Merri and Evans 2020), and the centrosaurine *Centrosaurus apertus*. The upper one-half of this assemblage zone also hosts the lambeosaurine *Lambeosaurus*, which continues up-section into the middle of the next zone.

Regarding *Corythosaurus*, a sub-adult of *C. casuarius* occurs in the lower DPFm ∼100 km east of DPP near Hilda (Evans 2007), and two specimens of *Corythosaurus* have been documented in the Coal Ridge Member of the Judith River Formation in Montana at Havre and Winifred (Takasaki et al. 2023). These finds suggest widespread distribution of the genus just above the Judith River–Belly River discontinuity and equivalent in age to the base of the DPFm at DPP (76.3 Ma; Rogers et al. 2023).

Of particular interest is the ceratopsid *Centrosaurus apertus,* for which two distinct taphonomic modes occur: multiple (∼20) football-field-sized monodominant bonebeds and multiple (∼20) isolated skulls/skeletons (Eberth and Getty 2005; Ryan and Evans 2005; Eberth et al. 2010; Brown 2013*a*; Brown et al. 2020). The taxon is also present in the Oldman and Dinosaur Park formations throughout southern Alberta. Eberth et al. (2010) documented bonebed occurences of *C. apertus* in the lower DPFm east of DPP along the South Saskatchewan River that correlate with those in the Park. Chiba et al. (2015) described both bonebed and isolated skull material of this species above the Comrey Sandstone Member (Troke 1993) of the OFm near Onefour (southeast Alberta). Whereas a diachronous contact between the Oldman and Dinosaur Park formations may explain occurrences of the taxon in different formations at about the same time (Chiba et al. 2015; its occurrence ∼160 km south of DPP suggests that the taxon was not sensitive to paleoenvironmental differences that may have existed between this area and DPP (Eberth and Hamblin 1993; Cullen and Evans 2016). Given the existing broad geographical distribution of the taxon across southern Alberta, paleothermometric data (Cullen and Evans 2016) that suggest long-distance migrations for this taxon, as well as its abundant occurrence in a variety of taphonomic modes, we hypothesize that *C. apertus* will eventually be discovered farther south in the Coal Ridge Member of the Judith River Formation of Montana, which lies chronostratigraphically above the Judith River–Belly River discontinuity and is thus equivalent in time to the DPFm at DPP (Rogers et al. 2023). If present there, it should be considered as a chronostratigraphic index taxon across a broad area of northern Laramidia.

Although previous work suggested that *Chasmosaurus russelli* and *Chasmosaurus belli* are stratigraphically separate (Godfrey and Holmes 1995; Ryan and Evans 2005; and Mallon et al. 2012), more recent work has resulted in both a less resolved specimen level taxonomy and locality data suggesting that the holotype of *C. russelli* (recovered from the Manyberries area of southeastern Alberta) equates to a position in the upper portion of the DPFm (Campbell et al. 2016, 2019; Fowler and Freedman-Fowler 2020). Accordingly, these observations reduce the current understanding of the stratigraphic occurrence of these taxa and their utility in defining assemblage zones or biochrons.

The assemblage zone also hosts abundant ankylosaur remains, though faunal changes in ankylosaur taxa within the DPFm are complex (Arbour and Currie 2013). The stratigraphic level of the holotype of *Euoplocephalus tutus* was not well described. Possible rediscovery of the site (Tanke, personal communication, 2022) in the lower part of the DPFm is currently being investigated. Lambe (1902) named the taxon *Stereocephalus tutus*, but the name was preoccupied and was renamed by Lambe (1910) as *Euoplocephalus tutus*. The majority of specimens (∼7) of this taxon are from the *Corythosaurus*–*Centrosaurus* assemblage zone, and only one specimen has been recovered from the lower part of the next younger assemblage zone (Arbour and Currie 2013). A second ankylosaurid species—*Dyoplosaurus acutosquameus*—is also known from the *Corythosaurus*–*Centrosaurus* assemblage zone on the basis of two specimens (Arbour and Currie 2013).

Prosaurolophus maximus–*Styracosaurus albertensis* assemblage zone (75.77–75.10 Ma)

This assemblage zone occurs within the middle one-third of the DPFm, 30–58 m above the base of the formation. Following Ryan and Evans (2005), we recognize the top of this assemblage zone as occurring "…at or near the Lethbridge Coal Zone…" and for stratigraphic convenience place the top of the zone at the base of the Lethbridge Coal Zone (58.25 m in the Iddesleigh section; Fig. 2), where the first prominent subbituminous coal occurs. The base of this zone is coincident in age with the top of the *Corythosaurus*–*Centrosaurus apertus* zone described above (75.77 + 0.29/−0.10 Ma). The age model extrapolates an age of 75.098 + 0.25/−0.063 Ma for the base of the Lethbridge Coal Zone and thus the top of this assemblage zone (Table 3; Fig. 3). The zone has a duration of approximately 672 ka.

The zone is characterized by the unique combination of the large hadrosaurine *Prosaurolophus maximus*, the centrosaurine *Styracosaurus albertensis*, and the chasmosaurine *Chasmosaurus belli*. In addition, some specimens of the lambeosaurine, *Lambeosaurus lambei*, are found in the lowest 20 m of this zone, thus straddling the boundary between this and the underlying assemblage zone. Finally, one specimen of the ankylosaur *Anodontosaurus lambei*, which is better known from the HCFm, has been recovered from this assemblage zone (Arbour and Currie 2013).

At least eight specimens assigned to *Prosaurolophus maximus* occur in the "upper" DPFm at the Park (Currie and Russell 2005), and although the taxon is not represented in the lowest 30 m of the DPFm—thus providing its biostratigraphic value—it is known to occur within the Lethbridge Coal Zone. Elsewhere in southern Alberta and Montana, the taxon ranges up-section well into the BFm (estimated age of ∼74 Ma; McGarrity et al. 2013; Drysdale et al. 2018; see discussion below). As with *Centrosaurus apertus*, *Styracosaurus albertensis* is characterized by both monodominant bonebeds ($n = \sim 3$) and multiple isolated skulls/skeletons ($n = \sim 10$), although in lower abundance (Brown 2013; Brown et al. 2020). While all currently recognized specimens of *Chasmosaurus belli* at DPP occur in this zone, taxonomic uncertainty has reduced the sample of clearly diagnostic specimens (Campbell et al. 2016, 2019; Fowler and Freedman-Fowler 2020; Holmes et al. 2020; see above).

Evans et al. (2014) documented the close association of the hadrosaurine *P. maximus* and the centrosaurine *S. albertensis* in the DPFm near Onefour, Alberta. In that area, U–Pb age data (Federico Fanti, personal communication, 2023) show that the base of the DPFm is younger than at DPP and indicate that the Onefour specimens fall within the age range proposed here for the dinosaur assemblage zone. Biostratigraphic evidence from the BFm indicates that *P. maximus* was coeval with *Baculites compressus*, lived during magnetochrons 33n.3n–33n.2n, and was broadly contemporaneous with specimens now referred to the taxon from the Two Medicine Formation of northwestern Montana (McGarrity et al. 2013; Drysdale et al. 2018). Because these occurrences show that *P. maximus* ranges through the overlying dinosaur assemblage zone (*Lambeosaurus magnicristus*–*Chasmosaurus irvinenensis*), it is likely of more limited biostratigraphic value than *S. albertensis*.

Lambeosaurus magnicristatus–pachyrhinosaur–*Chasmosaurus irvinensis* assemblage zone (75.10–74.44 Ma)

The base of this zone is coincident in age with the top of the *Prosaurolophus maximus*–*Styracosaurus albertensis* assemblage zone described above (75.098 + 0.25/−0.063 Ma). For stratigraphic convenience, the top of this zone is placed at the DPFm–BFm (nonmarine–marine) contact, with an inferred age of 74.44 + 0.30/−0.11 Ma (Table 3, Fig. 3). Thus, the zone has a minimum duration of approximately 658 ka. In the uppermost 21 m of the DPFm (Lethbridge Coal Zone; 58–79 m), most of the well-known megaherbivore taxa drop out and are replaced by rare taxa that are unknown elsewhere in the formation. These include the type specimen of the lambeosaurine *Lambeosaurus magnicristatus*, a pachyrhinosaur-like centrosaurine that resembles *Achelosaurus* (Ryan et al. 2010), and two specimens of the chasmosaurine *Chasmosaurus* (=*Vagaceratops*) *irvinensis*. *P. maximus* also persists into this interval, although in greatly reduced numbers (Drysdale et al. 2018; see above).

A referred specimen of *L. magnicristatus* was collected from near the base of the DPFm southeast of Manyberries, Alberta. As discussed above, this places this specimen at the same stratigraphic level as *Styracosaurus* and *P. maximus* in that area and suggests some degree of stratigraphic overlap between *L. magnicristatus* on the one hand and *Styracosaurus* and *P. maximus* on the other. *Chasmosaurus irvinensis* specimens have been found in exposures of the Lethbridge Coal Zone (DPFm) throughout southeastern Alberta. The holotype is from a locality near Medicine Hat, and two other specimens were collected near Onefour in southeastern Alberta (Campbell et al. 2019).

A comparison with dinosaur assemblage zones in the overlying Horseshoe Canyon Formation

The Campanian–Maastrichtian age HCFm of south-central Alberta has an age range of ∼5.1 Ma and encompasses three megaherbivore dinosaur assemblage zones (Eberth et al. 2013*a*; Eberth and Kamo 2020). In ascending stratigraphic order these are (1) the *Edmontosaurus regalis*–*Pachyrhinosaurus canadensis* zone, 73.1–71.5 Ma (duration ∼1.6 Myr), (2) the *Hypacrosaurus altispinus*–*Saurolophus osborni* zone, 71.5–69.6 Ma (duration 1.9 Myr), and (3) the *Eotriceratops xerinsularis* zone, 69.6–68.2 Ma (duration 1.4 Myr). In addition to the HCFm dinosaur assemblage zones exhibiting durations that are 2–3 times longer than those documented at DPP, their taxonomic compositions are less diverse (cf., Eberth et al. 2013*a*).

These data suggest that dinosaur assemblage-zone turnover rates decreased sharply from 74.4 to 73.1 Ma (latest Campanian) in western Canada and remained low (or decreased further) until the end-Cretaceous extinction event. This decrease in turnover rate is not merely due to patterns of overlapping occurrences within assemblages but is also seen independently in the duration of well-sampled, closely related individual taxa between the DPFm and HCFm:

1) *C. apertus* (∼0.6 Ma) and *S. albertensis* (∼0.5 Ma) versus *P. canadensis* (∼0.9 Ma);
2) *G. notabilis* (∼0.3 Ma) and *P. maximus* (∼0.5 Ma) versus *E. regalis* (∼0.7 Ma) and *S. osborni* (∼1.3 Ma); and
3) *C. casuarius* (∼0.3 Ma), *C. intermedius* (∼0.3 Ma), and *L. lambei* (∼0.5 Ma) versus *H. altispinus* (∼1.9 Ma).

Potential sampling biases notwithstanding, peak dinosaur diversity was achieved during the middle-to-late Campanian (Ramezani et al. 2022), the time interval recorded in the stratigraphic section at DPP. Thus, the recognition of peak dinosaur diversity is likely related in part to the relatively fast turnover rates that characterize taxa and assemblages at that time. Although the causes for declining megaherbivore-dinosaur turnover rates and assemblage diversity in western Canada during the Maastrichtian remain beyond the scope of this study, it is compelling to consider that the decline in turnover rates had begun by 73.1 Ma, shortly after the WIS had begun its final retreat from North America (Kauffman and Caldwell 1993). Accordingly, a decline in dinosaur assemblage turnover rates may have been a response to a decrease in environmental partitioning and the expansion of ecologically homogenous/stable nonmarine environments into the vast areas once occupied by the WIS, as suggested by the works of Horner et al. (1992), Brinkman et al. (1998), Gates et al. (2012), and Loewen et al. (2013).

Finally, it should be noted that for both the BRG and the Edmonton Group, the established assemblage zones are based on the occurrence of megaherbivores, specifically Ceratopsidae and Hadrosauridae. Similar zones either do not exist or have not yet been established for other large-bodied ornithischians (Ankylosauridae and Nodosauridae), for small-bodied ornithischians (e.g., Leptoceratopsidae, Pachycephalosauridae, and Thescelosauridae), for Tyrannosauridae, or for the several lineages of smaller theropods (e.g., Caenagnathidae, Dromaeosauridae, Ornithomimidae, and Troodontidae) (Eberth et al. 2013*a*; Funston 2020; Cullen et al. 2021). For some taxa, such as small-bodied ornithischians and small theropods, this pattern is likely largely driven by poor sampling (Brown et al. 2013*a*, 2013*b*; Evans et al. 2013). However, several theropod lineages are well sampled and show broad stratigraphic overlap of closely related species and/or widespread stratigraphic occurrences within the formation (Cullen et al. 2021). This may also represent a true distinction in species duration/replacement rates between ornithischian megaherbivores and contemporaneous theropod dinosaurs, suggesting distinct evolutionary rates, differing ecological sensitivities, contrasting levels of ecological partitioning, or a combination of several factors.

Summary and conclusions

Reproducible, high-precision radioisotopic ages have been difficult to obtain from DPP during the past 30 years. This problem is now being resolved with newly reported CA-ID-TIMS U–Pb geochronology of zircons from bentonite deposits distributed through the Park's exposed bedrock section. Five weighted mean U–Pb ages range from 76.718 ± 0.020 to 74.289 ± 0.014 Ma, indicating a duration of $\sim 2.429 \pm 0.024$ Myr for the exposed bedrock section. The reproducibility of these ages (within 2σ analytical error) has been demonstrated by independent CA-ID-TIMS U–Pb analyses of two of these bentonites (BB and PT) at different laboratories. These ages and the age-stratigraphic model that they support are the basis for geochronological calibration of the Park's rocks and fossils, as well as calibrations of biozones of microfossils, invertebrates, and vertebrates that have been developed at the Park and elsewhere. As additional radioisotopically calibrated stratigraphic sections from the BRG become available, we anticipate important advances in our understanding of the tectonic, basin evolution, and paleontological history of the region.

With respect to interpretations of the BRG's stratigraphic evolution in southern Alberta, our data reveal a sharp increase in rock accumulation rates at the base of the DPFm. This pattern broadly conforms to the widely accepted interpretation that the onset of transgression of the Bearpaw Sea was associated with increased accommodation resulting from a eustatic rise in sea level and an allogenic tectonic event in WIB. However, a very low rate of rock accumulation in the upper OFm exposed at DPP and a long-term and gradual decline in rock accumulation rates upward through the DPFm appear to reflect regionalized variations in tectonic activity, basin response, and sediment supply. By combining other radioisotopically calibrated and correlation of upper Campanian sections from other portions of the basin with our data (e.g., Wapiti Formation from west-central Alberta, OFm from southeastern and southwestern Alberta, Belly River Formation from western Saskatchewan, and Judith River Formation from north-central Montana), such interpretations can be tested and may provide clarity concerning the relative influences of changing sea-level, climate, and regionalized tectonics on basin architecture across the vast Judith River–Belly River wedge.

The resulting calibrations also reveal patterns of interest concerning the taxonomic composition and durations of some of the Park's biozones. For example, the newly calibrated dinosaur assemblage zones provide a basis for comparisons with data emerging from the Milk River drainage area at and south of the Canada–USA border. The unique taxonomic richness of the Park's dinosaur assemblage and the durations of its dinosaur assemblage zones can also be considered in a global geochronological context and compared closely with emerging data sets of finely calibrated dinosaur diversity patterns from other locations (e.g., Montana, New Mexico, and Utah). High-resolution chronostratigraphic frameworks from the Upper Cretaceous of North America can be combined now to refine patterns and frame questions concerning dinosaurian paleobiogeography, provincialism, migrations, and patterns of evolution and extinction in North America and Euro-Asia. Lastly, chronostratigraphic calibration of the Park's dinosaur assemblage zones confirms that during the last eight million years of the Cretaceous, megaherbivore turnover rates decreased notably, a pattern that may have been influenced by the final withdrawal of the WIS from North America and the establishment of vast areas of lowland terrestrial ecosystems.

Acknowledgements

Thanks to Craig Scott and the Royal Tyrrell Museum Cooperating Society for long-term financial and logistical support for this multi-decadal project. Special thanks to Eric Roberts for suggesting and coordinating a new way forward to resolve problems related to age comparisons of Campanian-age dinosaur-bearing strata of the Western Interior Basin and Alan Deino of the Berkeley Geochronology Center for his tireless efforts and patience in clarifying the ages of the Park's strata and dinosaurs. Bella Bennette is thanked for bentonite sample processing at MIT. Two anonymous reviewers and Associate Editor, Brian Pratt, provided insightful and helpful comments and criticisms that greatly improved the manuscript. We appreciate their attention to detail. DAE thanks all co-authors for their long-term commitment to this project.

Article information

History dates

Received: 24 March 2023
Accepted: 12 June 2023
Accepted manuscript online: 5 July 2023
Version of record online: 16 August 2023

Copyright

© 2023 The Crown and authors Eberth, Evans, Ramezani, Kamo, Currie, and Braman. This work is licensed under a Creative Commons Attribution 4.0 International License (CC BY 4.0), which permits unrestricted use, distribution, and reproduction in any medium, provided the original author(s) and source are credited.

Data availability

All data that support the interpretations and conclusions provided here are presented in the manuscript.

Author information

Author ORCIDs

David A. Eberth https://orcid.org/0009-0009-4671-7078

Author contributions

Conceptualization: DAE, DCE
Data curation: DAE, JR, SLK
Formal analysis: DAE, JR, SLK
Funding acquisition: DAE, JR
Investigation: DAE, CMB, PJC, DRB
Methodology: DAE, JR, SLK
Project administration: DAE
Visualization: DAE
Writing – original draft: DAE
Writing – review & editing: DAE, DCE, JR, SLK, CMB, PJC

Competing interests

The authors declare there are no competing interests.

Funding information

This research was supported by the US National Science Foundation grant EAR-1424892 to JR (S.A. Bowring); National Science and Engineering Council of Canada Grant RGPIN-2017-04715 to PJC; and Royal Tyrrell Museum Cooperating Society Research Funds provided to DAE.

References

Arbour, V.M., and Currie, P.J. 2013. *Euoplocephalus tutus* and the diversity of ankylosaurid dinosaurs in the Late Cretaceous of Alberta, Canada, and Montana, USA. PLoS ONE, **8**(5): e62421. doi:10.1371/journal.pone.0062421.

Barrett, P.M., McGowan, A.J., and Page, V. 2009, Dinosaur diversity and the rock record. Proceedings of the Royal Society B, **276**: 2667–2674. doi:10.1098/rspb.2009,0352.

Baszio, S. 1997a. Systematic palaeontology of isolated dinosaur teeth from the latest Cretaceous of south Alberta, Canada. *In* Investigations on Canadian dinosaurs. Courier Forschungsinstitut Senckenberg. Vol. **196**. pp. 33–77.

Baszio, S. 1997b. Palaeoecology of dinosaur assemblages throughout the Late Cretaceous of South Alberta, Canada. *In* Investigations on Canadian Dinosaurs. Courier Forschungsinstitut Senckenberg. Vol. **196**. pp. 1–31.

Beland, P., and Russell, D.A. 1978. Paleoecology of Dinosaur Provincial Park (Cretaceous), Alberta, interpreted from the distribution of articulated vertebrate skeletons. Canadian Journal of Earth Sciences, **15**: 1012–1024. doi:10.1139/e78-109.

Benton, M.A. 2008. How to find a dinosaur, and the role of synonymy in biodiversity studies. Paleobiology, **34**: 516–533. doi:10.1666/06077.1.

Beveridge, T.L., Roberts, E.M., Ramezani, J., Titus, A.L., Eaton, J.G., Irmis, R.B., and Sertich, J.J.W. 2022. Refined geochronology and revised stratigraphic nomenclature of the Upper Cretaceous Wahweap Formation, Utah, U.S.A. and the age of early Campanian vertebrates from southern Laramidia. Palaeogeography, Palaeoclimatology, Palaeoecology, **591**: 110876. doi:10.1016/j.palaeo.2022.110876.

Blum, M.D., and Tornquist, T.E. 2000. Fluvial responses to climate and sea-level change: a review and look forward. Sedimentology, **47**(supplement): 2–48. doi:10.1046/j.1365-3091.2000.00008.x.

Bowring, S.A., Schoene, B., Crowley, J.L., Ramezani, J., and Condon, D.J. 2006. High-precision U–Pb zircon geochronology and the stratigraphic record: progress and promise. *In* Geochronology: emerging opportunities. The Paleontological Society Papers. Vol. 12. *Edited by* T.D. Olszewski. pp. 25–45.

Braman, D.R. 2013. Triprojectate pollen occurrence in the Western Canada Sedimentary Basin and the group's global relationships. Contribution Series no. 1. Royal Tyrrell Museum of Palaeontology, Drumheller, AB. 538p.

Braman, D.R. 2018. Terrestrial palynostratigraphy of the Upper Cretaceous (Santonian) to lower Paleocene of southern Alberta, Canada. Palynology, **42**: 102–147. doi:10.1080/01916122.2017.1311958.

Braman, D.R., and Koppelhus, E.B. 2005. Campanian palynomorphs. *In* Dinosaur Provincial Park: a spectacular ancient ecosystem revealed. *Edited by* P.J. Currie and E.B. Koppelhus. Indiana University Press, Bloomington. pp. 101–130.

Brinkman, D.B. 1990. Paleoecology of the Judith River Formation (Campanian) of Dinosaur Provincial Park, Alberta, Canada: evidence from vertebrate microfossil localities. Palaeogeography, Palaeoclimatology, Palaeoecology, **78**: 37–54. doi:10.1016/0031-0182(90)90203-J.

Brinkman, D.B., Russell, A.P., and Peng, J.-H. 2005. Vertebrate microfossil sites and their contribution to studies of paleoecology. *In* Dinosaur Provincial Park: a spectacular ancient ecosystem revealed. *Edited by* P.J. Currie and E.B. Koppelhus. Indiana University Press, Bloomington. pp. 88–98.

Brinkman, D.B., Ryan, M.J., and Eberth, D.A. 1998. The paleogeographic and stratigraphic distribution of ceratopsids (Ornithischia) in the Upper Judith River Group of Western Canada. PALAIOS, **13**(2): 160–169. doi:10.2307/3515487.

Brown, C.M. 2013. Advances in quantitative methods in dinosaur palaeobiology: a case study in horned dinosaur evolution. Ph.D. thesis, University of Toronto, Toronto.

Brown, C.M., Evans, D.C, Campione, N.E., O'Brien, L.J., and Eberth, D.A. 2013a. Evidence for taphonomic size bias in the Dinosaur Park Formation (Campanian, Alberta), a model Mesozoic terrestrial alluvial–paralic system. Palaeogeography, Palaeoclimatology, Palaeoecology, **372**: 108–122. doi:10.1016j,palaeo.2012.06.027.

Brown, C.M., Evans, D.C., Ryan, M.J., and Russell, A.P. 2013b. New data on the diversity and abundance of small-bodied ornithopods (Dinosauria, Ornithischia) from the Belly River Group (Campanian) of Alberta. Journal of Vertebrate Paleontology, **33**: 495–520. doi:10.1080/02724634.2013.746229.

Brown, C.M., Holmes, R.B., and Currie, P.J. 2020. A subadult individual of *Styracosaurus albertensis* (Ornithischia: Ceratopsidae) with comments on ontogeny and intraspecific variation in *Styracosaurus* and *Centrosaurus*. Vertebrate Anatomy Morphology Palaeontology, **8**: 67–95. doi:10.18435/vamp29361.

Campbell, J.A., Ryan, M.J., Holmes, R.B., and Schröder-Adams, C. 2016. A re-evaluation of the Chasmosaurine Ceratopsid Genus *Chasmosaurus* (Dinosauria: Ornithischia) from the Upper Cretaceous (Campanian) Dinosaur Park Formation of Western Canada. PLoS ONE, **11**(1): e0145805. doi:10.1371/journal.pone.0145805.

Campbell, J.A., Ryan, M.J., Schroder-Adams, C.J., Holmes, R.B., and Evans, D.C. 2019. Temporal range extension and evolution of the chasmosaurine ceratopsid '*Vagaceratops*' *irvinensis* (Dinosauria: Ornithischia) in the Upper Cretaceous (Campanian) Dinosaur Park Formation of Alberta. Vertebrate Anatomy Morphology Palaeontology, **7**: 83–100. doi:10.18435/vamp29356.

Cant, D.J., and Stockmal, G.S. 1989. The Alberta foreland basin: relationship between stratigraphy and Cordilleran terrane-accretion events. Canadian Journal of Earth Sciences, **26**: 1964–1975. doi:10.1139/e89-166.

Carr, T.D., Varricchio, D.J., Sedlmayr, J.C., Roberts, E.M., and Moore, J.R. 2017. A new tyrannosaur with evidence for anagenesis and crocodile-like facial sensory system. Scientific Reports, **7**: 1–11. doi:10.1038/srep44942.

Catuneanu, O., and Sweet, A.R. 1999. Maastrichtian-Paleocene foreland-basin stratigraphies, western Canada: a reciprocal sequence architecture. Canadian Journal of Earth Sciences, **36**: 685–703. doi:10.1139/e98-018.

Chiba, K., Ryan, M.J., Eberth, D.A., Braman, D., Kobayashi, Y., and Evans, D.C., 2015. Taphonomy of a Centrosaurus apertus (Dinosauria: Ceratopsidae) bonebed from the Oldman Formation of Alberta, Canada. PALAIOS, **30**(9): 655–667.

Chiba, K., Ryan, M.J., Eberth, D.A., Braman, D., Kobayashi, Y., and Evans, D.C. 2015. Taphonomy of a *Centrosaurus apertus* (Dinosauria: Ceratopsidae) bonebed from the Oldman Formation of Alberta, Canada. PALAIOS, **30**(9): 655–667. doi:10.2110/palo.2014.084.

Clyde, W.C., Ramezani, J., Johnson, K.R., Bowring, S.A., and Jones, M.M. 2016. Direct high-precision U–Pb geochronology of the end-Cretaceous extinction and calibration of Paleocene astronomical timescales. Earth and Planetary Science Letters, **452**: 272–280. doi:10.1016/j.epsl.2016.07.041.

Cobban, W.A., Walaszczyk, I., Obradovich, J.D., and McKinney, K.C. 2006. A USGS zonal table for the Upper Cretaceous Middle Cenomanian–Maastrichtian of the western interior of the United States Based on Ammonites, Inoceramids, and radiometric ages. United States Geological Survey Open-File Report 2006-1250. Reston, VA.

Cullen, T.M., and Evans, D.C. 2016. Palaeoenvironmental drivers of vertebrate community composition in the Belly River Group (Campanian) of Alberta, Canada, with implications for dinosaur biogeography. BMC Ecology, **16**: 1–35. doi:10.1186/s12898-016-0106-8.

Cullen, T.M., Zanno, L., Larson, D.W., Todd, E., Currie, P.J., and Evans, D.C. 2021. Anatomical, morphometric, and stratigraphic analyses of theropod biodiversity in the Upper Cretaceous (Campanian) Dinosaur Park Formation. Canadian Journal of Earth Sciences, **58**(9): 870–884. doi:10.1139/cjes-2020-0145.

Cúneo, R., Ramezani, J., Scasso, R., Pol, D., Escapa, I., Zavattieri, A.M., and Bowring, S.A. 2013. High-precision U–Pb geochronology and a new chronostratigraphy for the Cañadón Asfalto Basin, Chubut, central Patagonia: implications for terrestrial faunal and floral evolution in Jurassic. Gondwana Research, **24**: 1267–1275. doi:10.1016/j.gr.2013.01.010.

Currie, P.J., and Koppelhus, E.B. (*Editors*). 2005. Dinosaur Provincial Park: a spectacular ancient ecosystem revealed. University of Indiana Press, Bloomington. 648p.

Currie, P.J. 2003. Cranial anatomy of tyrannosaurid dinosaurs from the Late Cretaceous of Alberta, Canada. Acta. Palaeontologica Polonica **48**(2): 191–226.

Currie, P.J. 2005. History of research. *In* Dinosaur Provincial Park: a spectacular ancient ecosystem revealed. *Edited by* P.J. Currie and E.B. Koppelhus. Indiana University Press, Bloomington. pp. 3–33.

Currie, P.J., and Russell, D.A. 2005. The geographic and stratigraphic distribution of articulated and associated dinosaur remains *In* Dinosaur Provincial Park: a spectacular ancient ecosystem revealed. University of Indiana Press, Bloomington. pp. 537–569.

Cuthbertson, R.S., and Holmes, R.B. 2010. The first complete description of the holotype of *Brachylophosaurus canadensis* Sternberg, 1953 (Dinosauria: Hadrosauridae) with comments on intraspecific variation. Zoological Journal of the Linnean Society, **159**: 373–397. doi:10.1111/j.1096-3642.2009.00612.x.

Deino, A.L, and Potts, R. 1990. Single crystal $^{40}Ar/^{39}Ar$ dating of the Olorgesailie Formation, southern Kenya rift. Journal of Geophysical Research, **95**(B6): 8453–8470. doi:10.1029/JB095iB06p08453.

Deino, A.L., Scott, G., Saylor, B., Mulugeta, A., Angelini, J.D., and Haile-Selassie, Y. 2010. $^{40}Ar/^{39}Ar$ dating, paleomagnetism, and tephrochemistry of Pliocene strata of the hominid-bearing Woranso–Mille area, west-central Afar Rift, Ethiopia. Journal of Human Evolution, **58**: 111–126. doi:10.1016/j.jhevol.2009.11.001.

Drysdale, E.T, Therrien, F., Zelenitsky, D.K., Weishampel, D.B., and Evans, D.C. 2018. Description of juvenile specimens of *Prosaurolophus maximus* (Hadrosauridae: Saurolophinae) from the Upper Cretaceous Bearpaw Formation of southern Alberta, Canada, reveals ontogenetic changes in crest morphology. Journal of Vertebrate Paleontology, **38**: e1547310. doi:10.1080/02724634.2018.1547310.

Eberth, D.A. (*Compiler and Editor*). 2017. Campanian–Maastrichtian dinosaurs and environments at Dinosaur Provincial Park and Drumheller, Alberta, Canada. *In* Pre-conference Field Trip Guidebook. Proceedings of the 77th Annual Meeting of the Society of Vertebrate Paleontology. 70 p.

Eberth, D., Brinkman, D.B., and Barkas, V. 2010. A centrosaurine megabonebed from the Upper Cretaceous of southern Alberta: implications for behaviour and death events. *In* New Perspectives on Horned Dinosaurs: The Royal Tyrrell Museum Ceratopsian Symposium. *Edited by* M.J. Ryan, B.J. Chinnery-Allgeier and D.A. Eberth. Indiana University Press, Bloomington. pp. 495–508.

Eberth, D.A. 2015. Origins of dinosaur bonebeds in the Cretaceous of Alberta, Canada. Special Issue: Papers Commemorating the 30 Anniversary of the Royal Tyrrell Museum of Palaeontology. Vol. 52. *Edited by* J.D. Gardner, D.M. Henderson and F. Therrien. pp. 655–681. doi:10.1139/cjes-2014-0200.

Eberth, D.A. Stratigraphic architecture of the Belly River Group (Campanian) in the plains of southern Alberta: revisions and updates to an existing model, and implications for correlating dinosaur-rich strata. PLoS ONE. In press.

Eberth, D.A., 2005. The geology. *In* Dinosaur Provincial Park: a spectacular ancient ecosystem revealed. *Edited by* P.J. Currie and E.B. Koppelhus. Indiana University Press, Bloomington. pp. 54–82.

Eberth, D.A., and Braman, D.R. 2012. A revised stratigraphy and depositional history for the Horseshoe Canyon Formation (Upper Cretaceous), southern Alberta plains. Canadian Journal of Earth Sciences, **49**: 1053–1086. doi:10.1139/e2012-035.

Eberth, D.A., and Currie, P.J. 2005. Vertebrate taphonomy and taphonomic modes. *In* Dinosaur Provincial Park: a spectacular ancient ecosystem revealed. *Edited by* P.J. Currie and E.B. Koppelhus. Indiana University Press, Bloomington. pp. 453–477.

Eberth, D.A., and Deino, A.L. 1992. A geochronology of the non-marine Judith River Formation of southern Alberta. Proceedings of the SEPM 1992 Theme Meeting. Fort Collins, CO. pp. 24–25.

Eberth, D.A., and Deino, A.L. 2005. New ^{40}Ar/^{39}Ar ages from three bentonites in the Bearpaw, Horseshoe Canyon, and Scollard formations (Upper Cretaceous–Paleocene) of southern Alberta, Canada. *In* Abstracts Volume for the Dinosaur Provincial Park Symposium. Special Publication of the Royal Tyrrell Museum. *Edited by* D.R. Braman, F. Therrien, E.B. Koppelhus and W. Taylor. Royal Tyrrell Museum. pp. 23–24.

Eberth, D.A., and Evans, D.C. 2011. Geology and palaeontology of Dinosaur Provincial Park, Alberta. *In* International Hadrosaur Symposium Field Trip Guidebook. Special Publication. Royal Tyrrell Museum, Drumheller, AB. 52p.

Eberth, D.A., and Getty, M.A. 2005. Ceratopsian bonebeds: occurrences, origins and significance. *In* Dinosaur Provincial Park: a spectacular ancient ecosystem revealed. *Edited by* P.J. Currie and E.B. Koppelhus. Indiana University Press, Bloomington. pp. 501–536.

Eberth, D.A., and Hamblin, A.P. 1993. Tectonic, stratigraphic, and sedimentologic significance of a regional discontinuity in the upper Judith River Group (Belly River Wedge) of southern Alberta, Saskatchewan, and northern Montana. Canadian Journal of Earth Sciences, **30**: 174–200. doi:10.1139/e93-016.

Eberth, D.A., and Kamo, S.L. 2019. First high-precision U–Pb CA–ID–TIMS age for the Battle Formation (Upper Cretaceous), Red Deer River valley, Alberta, Canada: implications for ages, correlations, and dinosaur biostratigraphy of the Scollard, Frenchman, and Hell Creek formations. Canadian Journal of Earth Sciences, **56**: 1041–1051. doi:10.1139/cjes-2018-0098.

Eberth, D.A., and Kamo, S.L. 2020. High-precision U–Pb CA–ID–TIMS dating and chronostratigraphy of the dinosaur-rich Horseshoe Canyon Formation (Upper Cretaceous, Campanian–Maastrichtian), Red Deer River valley, Alberta, Canada. Canadian Journal of Earth Sciences, **57**: 1220–1237. doi:10.1139/cjes-2019-0019.

Eberth, D.A., Braman, D.R., and Tokaryk, T.T. 1990. Stratigraphy, sedimentology and vertebrate paleontology of the Judith River Formation (Campanian) near Muddy Lake, west-central Saskatchewan. Bulletin of Canadian Petroleum Geology, **38**: 387–406.

Eberth, D.A., Currie, P.J., Brinkman, D.B., Ryan, M.J., Braman, D.R., Gardner, J.D., et al. 2001. Alberta dinosaurs and other fossil vertebrates: Judith River and Edmonton groups (Campanian–Maastrichtian). *In* Guidebook for the field trips. (Society of Vertebrate Paleontology 61st Annual Meeting—Mesozoic and Cenozoic Paleontology in the Western Plains and Rocky Mountains). Museum of the Rockies Occasional Paper 3. *Edited by* C.L. Hill. pp. 49–75.

Eberth, D.A., Evans, D.C., Brinkman, D.B., Therrien, F., Tanke, D.H., and Russell, L.S. 2013a. Dinosaur biostratigraphy of the Edmonton Group (Upper Cretaceous), Alberta, Canada: evidence for climate influence. Canadian Journal of Earth Sciences, **50**(7): 701–726. doi:10.1139/cjes-2012-0185.

Eberth, D.A., Roberts, E.M., Deino, A.L., Bowring, S.A., and Ramezani, J. 2013b. Twenty-three years of radiometric dating at Dinosaur Provincial Park (Upper Cretaceous, Alberta, Canada). *In* Society of Vertebrate Paleontology, Annual Meeting (Los Angeles), Program and Abstracts. p. 120.

Eberth, D.A., Thomas, R.B, and Deino, A. 1992. Preliminary K–Ar dates from bentonites in the Judith River and Bearpaw Formations (Upper Cretaceous) of Dinosaur Provincial Park, southern Alberta, Canada. *In* Aspects of nonmarine Cretaceous geology. Proceedings of the Conference on Nonmarine Cretaceous Correlations, Urumqi, China, 1987. *Edited by* N. Mateer and P.J. Chen. China Ocean Press, Beijing. pp. 296–304.

Evans, D.C. 2007. Ontogeny and evolution of lambeosurine dinosaurs (Ornithischia: Hadrosauridae). Ph.D. thesis, University of Toronto, Toronto, ON. 529p.

Evans, D.C., and Reisz, R.R. 2007. Anatomy and relationships of *Lambeosarus magnicristatus*, a crested hadrosaurid dinosaur (Ornithischia) from the Dinosaur Park Formation, Alberta. Journal of Vertebrate Paleontology, **27**: 373–393. doi:10.1671/0272-4634(2007)27%5b373:AAROLM%5d2.0.CO;2.

Evans, D.C., Bavington, R., and Campione, N.E. 2009. An unusual hadrosaurid braincase from the Dinosaur Park Formation and the biostratigraphy of *Parasaurolophus* (Ornithischia: Lambeosaurinae) from southern Alberta. Canadian Journal of Earth Sciences, **46**: 791–800. doi:10.1139/E09-050.

Evans, D.C., McGarrity, C.T., and Ryan, M.J. 2014. A skull of *Prosaurolophus maximus* (Hadrosauridae), and the spaciotemporal distribution of faunal zones in the Dinosaur Park Formation, Alberta. *In* The Hadrosaurs: Proceedings of the International Hadrosaur Symposium. *Edited by* D.A. Eberth and D.C. Evans. Indiana University Press, Bloomington. pp. 200–207.

Evans, D.C., Schott, R.K., Larson, D.W., Brown, C.M., and Ryan, M.J. 2013. The oldest North American pachycephalosaurid and the hidden diversity of small-bodied ornithischian dinosaurs. Nature Communications, **4**: 1828. doi:10.1038/ncomms2749.

Foreman, B., Rogers, R.R., Deino, A.L., Wirth, K.R., and Thole, J.T. 2008. Geochemical characterization of bentonite beds in the Two Medicine Formation (Campanian, Montana), including a new ^{40}Ar/^{39}Ar age. Cretaceous Research, **29**: 373–385. doi:10.1016/j.cretres.2007.07.001.

Fowler, D.W. 2017. Revised geochronology, correlation, and dinosaur stratigraphic ranges of the Santonian–Maastrichtian (Late Cretaceous) formations of the Western Interior of North America. PLoS ONE, **12**(11): e0188426. doi:10.1371/journal.pone.0188426.

Fowler, D.W., and Freedman-Fowler, E.A. 2020. Transitional evolutionary forms in chasmosaurine ceratopsid dinosaurs: evidence from the Campanian of New Mexico. PeerJ, **8**: e9251. doi:10.7717/peerj.9251.

Freedman-Fowler, E.A., and Horner, J.R. 2015. A new brachylophosaurin hadrosaur (Dinosauria: Ornithischia) with an intermediate nasal crest from the Campanian Judith River Formation of northcentral Montana. PLoS ONE, **10**(11): e0141304. doi:10.1371/journal.pone.0141304.

Funston, G.F. 2020. Caenagnathids of the Dinosaur Park Formation (Campanian) of Alberta, Canada: anatomy, osteo-histology, taxonomy, and evolution. Vertebrate Anatomy Morphology Palaeontology, **8**: 105–153. doi:10.18435/vamp29362.

Gale, A.S., Mutterlose, J., Batenburg, S., Gradstein, F.M., Agterberg, F.P., Ogg, J.G., and Petrizzo, M.R. 2020. Chapter 27—the Cretaceous period. *In* Geologic time scale 2020. *Edited by* F.M. Gradstein, J.G. Ogg, M.D. Schmitz and G.M. Ogg. Elsevier. pp. 1023–1086. doi:10.1016/B978-0-12-824360-2.00027-9.

Gastaldo, R.A., Neveling, J., Geissman, J.W., and Kamo, S.L. 2018. A lithostratigraphic and magnetostratigraphic framework in a geochronologic context for a purported Permian–Triassic boundary section at Old (West) Lootsberg Pass, Karoo Basin, South Africa. Geological Society of America Bulletin, **130**: 1411–1438. doi:10.1130/B31881.1.

Gates, T.A., Prieto-Marquez, A., and Zanno, L.E. 2012. Mountain building triggered Late Cretaceous North American megaherbivore dinosaur radiation. PLoS ONE, **7**(8): e42135. doi:10.1371/journal.pone.0042135.

Godfrey, S.J., and Holmes, R.B. 1995. Cranial morphology and systematics of *Chasmosaurus* (Dinosauria: Ceratopsidae) from the Upper Cretaceous of western Canada. Journal of Vertebrate Paleontology, **15**(4): 726–742. doi:10.1080/02724634.1995.10011258.

Goodwin, M.B, and Deino, A.L. 1989. The first radiometric ages from the Judith River Formation (Upper Cretaceous), Hill County, Montana. Canadian Journal of Earth Sciences, **26**: 1384–1391. doi:10.1139/e89-118.

Hamblin, A.P. 1997. Regional distribution and dispersal of the Dinosaur Park Formation, Belly River Group, surface and subsurface of southern Alberta. Bulletin of Canadian Petroleum Geology, **45**(3): 377–399.

Hamblin, A.P., and Abrahamson, B.W. 1996. Stratigraphic architecture of "Basal Belly River" cycles, Foremost Formation Belly River Group, subsurface of southern Alberta and southwestern Saskatchewan. Bulletin of Canadian Petroleum Geology, **44**: 654–673.

Haslett, J., and Parnell, A. 2008. A simple monotone process with application to radiocarbon dated depth chronologies. Journal of the Royal Statistical Society: Series C, **57**: 399–418.

Henderson, D.M, and Tanke, D.H. 2010. Estimating past and future dinosaur skeletal abundances in Dinosaur Provincial Park, Alberta, Canada. Canadian Journal of Earth Sciences, **47**: 1291–1304. doi:10.1139/E10-033.

Hiess, J., Condon, D.J., McLean, N., and Noble, S.R. 2012. ^{238}U/^{235}U systematics in terrestrial uranium-bearing minerals. Science, **335**(6076): 1610–1614.

Holmes, R.B., Forster, C.A., Ryan, M.J., and Shepherd, K.M. 2001. A new species of *Chasmosaurus* from the Dinosaur Park Formation of Southern Alberta. Canadian Journal of Earth Sciences, **38**: 1423–1438. doi:10.1139/e01-036.

Holmes, R.B., Persons, W.S., Rupal, B.S., Qureshi, A.J., and Currie, P.J. 2020. Morphological variation and asymmetrical development in the skull of *Styracosaurus albertensis*. Cretaceous Research, **107**: 104308. doi:10.1016/j.cretres.2019.104308.

Horner, J., Varricchio, D.J., and Goodwin, M.B. 1992. Marine transgressions and the evolution of Cretaceous dinosaurs. Nature, **358**: 59–61. doi:10.1038/358059a0.

Jaffey, A.H., Flynn, K.F., Glendenin, L.E., Bentley, W.C., and Essling, A.M. 1971. Precision measurement of half-lives and specific activities of ^{235}U and ^{238}U. Physical Review, **4**: 1889–1906.

Jerzykiewicz, T, and Norris, D.K. 1994. Stratigraphy, structure and syntectonic sedimentation of the Campanian 'Belly River' clastic wedge in the southern Canadian Cordillera. Cretaceous Research, **15**: 367–399. doi:10.1006/cres.1994.1022.

Jinnah, Z.A., Roberts, E.M., Deino, A.L., Larsen, J., and Link, P.K. 2009. New ^{40}Ar/^{39}Ar and detrital zircon U–Pb ages for the Upper Cretaceous Wahweap and Kaiparowits formations on the Kaiparowits Plateau, Utah: implications for regional correlation, provenance, and biostratigraphy. Cretaceous Research, **30**: 287–299. doi:10.1016/j.cretres.2008.07.012.

Kauffman, E.G., and Caldwell, W.G.E. 1993. The Western Interior Basin in space and time. *In* Evolution of the Western Interior Basin. *Edited by* E.G. Kauffman and W.G.E. Caldwell. Geological Association of Canada, Special Paper. Vol. **39**. pp. 1–30.

Kuiper, K.F., Deino, A.L., Hilgen, F.J., Krijgsman, W., Renne, P.R., and Wijbrans, J.R. 2008. Synchronizing rock clocks of Earth history. Science, **320**: 500–504. doi:10.1126/science.1154339.

Lambe, L.M. 1902. New genera and species from the Belly River Series (mid-Cretaceous). *In* Contributions to Canadian palaeontology. Geological Survey of Canada. pp. 25–81.

Lambe, L.M. 1910. Note on the parietal crest of *Centrosaurus apertus* and a proposed new generic name for *Stereocephalus tutus*. Ottawa Naturalist, **14**: 149–151.

Legarreta, L., and Uliana, M.A. 1998. Anatomy of hinterland depositional sequences: Upper Cretaceous fluvial strata, Neuquen Basin, West-Central Argentina. *In* Relative role of eustasy, climate, and tectonism in continental rocks. Special Publication. Vol. 59. *Edited by* K.W. Shanley and P.J. McCabe. SEPM. pp. 83–92

Lehman, T.M. 1997. Late Campanian dinosaur biogeography in the western interior of North America. *In* Proceedings of the Dinofest International. *Edited by* D.L. Wolberg, E. Stump and G.D. Rosenberg. Academy of Natural Sciences, Philadelphia. pp. 223–240.

Lehman, T.M. 2001. Late Cretaceous *dinosaur* provinciality. *In* Mesozoic vertebrate life. *Edited by* D.H. Tanke and K. Carpenter. Indiana University Press. pp. 310–328.

Lerbekmo, J.F. 1989. The stratigraphic position of the 33-33r (Campanian) polarity chron boundary in southeastern Alberta. Bulletin of Canadian Petroleum Geology, **37**: 43–47.

Lerbekmo, J.F. 2002. The Dorothy bentonite: and extraordinary case of secondary thickening in a late Campanian volcanic ash fall in central Alberta. Canadian Journal of Earth Sciences, **39**: 1745–1754. doi:10.1139/e02-079.

Lerbekmo, J.F. 2005. Paleomagnetostratigraphy. *In* Dinosaur Provincial Park: a spectacular ancient ecosystem revealed. *Edited by* P.J. Currie and E.B. Koppelhus. Indiana University Press, Bloomington. pp. 83–87.

Loewen, M.A., Irmis, R.B., Sertich, J.J., Currie, P.J., and Sampson, S.D. 2013. Tyrant dinosaur evolution tracks the rise and fall of Cretaceous oceans. PLoS ONE, **8**(11): e79420. doi:10.1371/journal.pone.0079420.

Lowi-Merri, T.M., and Evans, D.C. 2020. Cranial variation in *Gryposaurus* and biostratigraphy of hadrosaurines (Ornithischia: Hadrosauridae) from the Dinosaur Park Formation of Alberta, Canada. Canadian Journal of Earth Sciences, **57**(6): 765–779. doi:10.1139/cjes-2019-0073.

Mallon, J.C., Evans, D.C, Ryan, M.J., and Anderson, J.S. 2012. Megaherbivorous dinosaur turnover in the Dinosaur Park Formation (upper Campanian) of Alberta, Canada. Palaeogeography, Palaeoclimatology, Palaeoecology, **350-352**: 124. doi:10.1016/j.palaeo.2012.06.024.

McGarrity, C., Campione, N., and Evans, D.C. 2013. Cranial anatomy and variation in *Prosaurolophus maximus* (Dinosauria: Hadrosauridae). Zoological Journal of the Linnean Society, 167. doi:10.1111/zoj.12009

Min, K.W., Renne, P.R., and Huff, W.D. 2001. ^{40}Ar/^{39}Ar dating of Ordovician K-bentonites in Laurentia and Baltoscandia. Earth and Planetary Science Letters, **185**: 121–134. doi:10.1016/S0012-821X(00)00365-4.

Obradovich, J.D. 1993. A Cretaceous time scale. *In* Evolution of the Western Interior Basin. Special Paper 39. *Edited by* W.G.E. Caldwell and E.G. Kauffman. Geological Association of Canada. pp. 379–396.

Ogg, J.G., Agterberg, F.P., and Gradstein, F.M. 2004. The Cretaceous period. *In* A geologic time scale 2004. *Edited by* F.M. Gradstein, J.G. Ogg and A. Smith. Cambridge University Press, Cambridge. pp. 344–383.

Ogg, J.G., and Hinnov, L.A. 2012. Cretaceous. *In* The geologic time scale 2012. *Edited by* F.M. Gradstein, J.G. Ogg, M.D. Schmitz and G.M. Ogg. Elsevier, Amsterdam. pp. 793–853.

Parnell, A.C., Haslett, J., Allen, J.R.M., Buck, C.E., and Huntley, B. 2008. A flexible approach to assessing synchroneity of past events using Bayesian reconstructions of sedimentation history. Quaternary Science Reviews, **27**: 1872–1885.

Penkalski, P. 2013. A new ankylosaurid from the late Cretaceous Two Medicine Formation of Montana, USA. Acta Palaeontologica Polonica. doi:10.4202/app.2012.0125.

Penkalski, P., and Blows, W.T. 2013. *Scolosaurus cutleri* from the Dinosaur Park Formation of Alberta, Canada. Canadian Journal of Earth Sciences, **50**: 171–182. doi:10.1139/cjes-2012-0098.

Phillips, D., and Matchan, E.L. 2013. Ultra-high precision ^{40}Ar/^{39}Ar ages for Fish Canyon Tuff and Alder Creek Rhyolite sanidine: new dating standards required? Geochimica et Cosmochimica Acta, **121**: 229–239. doi:10.1016/j.gca.2013.07.003.

Price, R.A. 1994. Cordilleran tectonics and the evolution of the Western Canada Sedimentary Basin. *In* Geological atlas of the Western Canada Sedimentary Basin. *Edited by* G.D. Mossop and I. Shetsen. Alberta Geological Survey and Canadian Society of Petroleum Geology, Edmonton. pp. 1322.

Prieto-Marquez, A. 2005. New information on the cranium of *Brachylophosaurus canadensis* (Dinosauria, Hadrosauridae), with a revision of its phylogenetic position. Journal of Vertebrate Paleontology, **25**: 144–156. doi:10.1671/0272-4634(2005)025%5b0144:NIOTCO%5d2.0.CO;2.

Prieto-Marquez, A., and Carpenter, K. 2007. Postcranial osteology of the hadrosaurid dinosaur *Brachylophosaurus canadensis* from the Late Cretaceous of Montana. *In* Horns and beaks. Ceratopsian and ornithopod dinosaurs. *Edited by* K. Carpenter. Indiana University Press, Bloomington. pp. 91–115.

Ramezani, J., Beveridge, T.L., Rogers, R.R., Eberth, D.A., and Roberts, E.M. 2022. Calibrating the zenith of dinosaur diversity in the Campanian of the Western Interior Basin by CA-ID-TIMS U–Pb geochronology. Scientific Reports, **12**: 16026. doi:10.1038/s41598-022-19896-w.

Ramezani, J., Fastovsky, D.E., and Bowring, S.A. 2014. Revised chronostratigraphy of the Lower Chinle Formation strata in Arizona and New Mexico (USA): high-precision U–Pb geochronological constraints on the Late Triassic evolution of dinosaurs. American Journal of Science, **314**: 981–1008. doi:10.2475/06.2014.01.

Renne, P.R., Balco, G., Ludwig, K.R., Mundil, R., and Min, K. 2011. Response to the comment by W.H. Schwartz et al. on "Joint determinations of ^{40} K decay constants and ^{40}Ar∗/^{39}Ar for the Fish Canyon sanidine standard, and improved accuracy for ^{40}Ar/^{39}Ar geochronology" by P.R. Renne et al. (2010). Geochimica et Cosmochimica Acta, **75**: 5097–5100. doi:10.1016/j.gca.2011.06.021.

Renne, P.R., Deino, A.L., Walter, R.C, Turrin, B.D., Swisher, C.C., Becker, T.A., et al. 1994. Intercalibration of astronomical and radioisotopic time. Geology, **22**: 783–786. doi:10.1130/0091-7613(1994)022%3c0783:IOAART%3e2.3.CO;2.

Renne, P.R., Mundil, R., Balco, G., Min, K., and Ludwig, K.R. 2010. Joint determination of ^{40}K decay constants and ^{40}Ar∗/^{39}Ar for the Fish Canyon sanidine standard, and improved accuracy for ^{40}Ar/^{39}Ar geochronology. Geochimica et Cosmochimica Acta, **74**: 5349–5367. doi:10.1016/j.gca.2010.06.017.

Renne, P.R., Swisher, C.C., Deino, A.L., Karner, D.B., Owens, T.L., and DePaolo, D.J. 1998. Intercalibration of standards, absolute ages and uncertainties in ^{40}Ar/^{39}Ar dating. Chemical Geology, **145**: 117–152. doi:10.1016/S0009-254 1(97)00159-9.

Roberts, E.M., Deino, A.L., and Chan, M.A. 2005. ^{40}Ar/^{39}Ar age of the Kaiparowits Formation, southern Utah, and correlation of contemporaneous Campanian strata and vertebrate faunas along the margin of the Western Interior Basin. Cretaceous Research, **26**: 307–318. doi:10.1016/j.cretres.2005.01.002.

Roberts, E.M., Sampson, S.D., Deino, A.L., Bowring, S.A., and Buchwaldt, R. 2013. The Kaiparowits Formation: a remarkable record of Upper Cretaceous terrestrial ecosystems, evolution and tectonics in Western North America. *In* The Late Cretaceous of Southern Utah: at the top of the Grand Staircase. *Edited by* A. Titus and M.A. Loewen. Indiana University Press, Bloomington. pp. 85–106.

Rogers, R.R. 1990. Taphonomy of three dinosaur bone beds in the Upper Cretaceous Two Medicine Formation of northwestern Montana: evidence for drought related mortality. PALAIOS, **5**: 394–413. doi:10.2307/3514834.

Rogers, R.R., Eberth, D.A., and Ramezani, J. 2023. The "Judith River-Belly River Problem" revisited: new perspectives on the correlation of Campanian dinosaur-bearing strata in Montana and Alberta based on a revised stratigraphic model updated with CA-ID-TIMS U–Pb geochronology. Geological Society of America Bulletin, **v**: xxx–xxx. doi:10.1130/B36999.1.

Rogers, R.R., Kidwell, S.M., Deino, A.L., Mitchell, J.P., Nelson, K., and Thole, J.T. 2016. Age, correlation, and lithostratigraphic revision of the Upper Cretaceous (Campanian) Judith River Formation in its type area (north-central Montana), with a comparison of low- and high-accommodation alluvial records The Journal of Geology, **124**: 99–135. doi:10.1086/684289.

Rogers, R.R., Swisher, C.C., II, and Horner, J.R. 1993. ^{40}Ar/^{39}Ar age and correlation of the nonmarine Two Medicine Formation (Upper Cretaceous), northwestern Montana, U.S.A. Canadian Journal of Earth Sciences, **30**: 1066–1075. doi:10.1139/e93-090.

Russell, L.S. 1983. Evidence for an unconformity at the Scollard-Battle contact, Upper Cretaceous strata, Alberta. Canadian Journal of Earth Sciences, **20**: 1219–1231. doi:10.1139/e83-109.

Ryan, M.J., and Evans, D.C. 2005. Ornithischian dinosaurs. *In* Dinosaur Provincial Park: a spectacular ancient ecosystem revealed. *Edited by* P.J. Currie and E.B. Koppelhus. Indiana University Press, Bloomington. pp. 312–348.

Ryan, M.J., and Russell, A.P. 2001. Dinosaurs of Alberta (exclusive of Aves). *In* Mesozoic vertebrate life. *Edited by* D.H. Tanke and K. Carpenter. Indiana University Press, Bloomington. pp. 279–297.

Ryan, M.J., and Russell, A.P. 2005. A new centrosaurine ceratopsid from the Oldman Formation of Alberta and its implications for centrosaurine taxonomy and systematics. Canadian Journal of Earth Sciences, **42**: 1369–1387. doi:10.1139/e05-029.

Ryan, M.J., Eberth, D.A., Brinkman, D.B., Currie, P.J., and Tanke, D.H. 2010. A new *Pachyrhinosaurus*-like ceratopsid from the upper Dinosaur Park Formation (Late Campanian) of southern Alberta, Canada. *In* New Perspectives on Horned Dinosaurs: The Royal Tyrrell Museum Ceratopsian Symposium. *Edited by* M.J. Ryan, B.J. Chinnery-Allgeier and D.A. Eberth. Indiana University Press, Bloomington. pp. 141–155.

Ryan, M.J., Evans, D.C., and Shepherd, K.M. 2012. A new ceratopsid from the Foremost Formation (middle Campanian) of Alberta. Canadian Journal of Earth Sciences, **49**: 1251–1262. doi:10.1139/e2012-056.

Sampson, S.D., Loewen, M.A., Farke, A.A., Roberts, E.M., Forster, C.A., Smith, J.A., and Titus, A.L. 2010. New horned dinosaurs from Utah provide evidence for intracontinental dinosaur endemism. PLoS ONE, **5**: e12292. doi:10.1371/journal.pone.0012292.

Shanley, K.W., and McCabe, P.J. 1998. Relative role of eustasy, climate, and tectonism in continental rocks, an introduction. *In* Relative role of eustasy, climate, and tectonism in continental rocks. Special Publication. Vol. 59. *Edited by* K.W. Shanley and P.J. McCabe. SEPM. pp. iii–iix.

Sternberg, C.M. 1950. Map 969A. Geological Survey of Canada, Steveville.

Takasaki, R., Chiba, K., Fiorillo, A.R., Brink, K.S., Evans, D.C., Fanti, F., et al. 2023. Description of the first definitive *Corythosaurus* (Dinosauria, Hadrosauridae) specimens from the Judith River Formation in Montana, USA and their paleobiogeographical significance. The Anatomical Record. **306**: 1918–1938. doi:10.1002/ar.25097. PMID: 36273398.

Thomas, R.G, Eberth, D.A., Deino, A.L., and Robinson, D. 1990. Composition, radioisotopic ages, and potential significance of an altered volcanic ash (bentonite) from the Upper Cretaceous Judith River Formation, Dinosaur Provincial Park, southern Alberta, Canada. Cretaceous Research, **11**: 125–162. doi:10.1016/S0195-6671(05)80030-8.

Troke, C.G. 1993. Sedimentology, stratigraphy and calcretes of the Comrey Member, Oldman Formation (Campanian), Milk River Canyon, southeastern Alberta. M.Sc. thesis, University of Calgary, Calgary. 146p.

Tsujita, C.J. 1995. Stratigraphy, taphonomy, and paleoecology of the Upper Cretaceous Bearpaw Formation in southern Alberta. Ph.D. thesis, McMaster University, Hamilton, ON. 356p.

Tweet, J.S., Chin, K., Braman, D.R., and Murphy, N.L. 2008. Probable gut contents within a specimen of *Brachylophosaurus canadensis* (Dinosauria: Hadrosauridae) from the Upper Cretaceous Judith River Formation of Montana. PALAIOS, **23**: 624–635. doi:10.2110/palo.2007.p07-044r.

Wang, S.C., and Dodson, P. 2006. Estimating the diversity of dinosaurs. Proceedings of the National Academy of Sciences of the United States of America, **103**(37): 13601–13605. doi:10.1073/pnas.0606028103.

Warshaw, E.A., and Fowler, D.W. 2022. A transitional species of *Daspletosaurus* Russell, 1970 from the Judith River Formation of eastern Montana. PeerJ, **10**: e14461. doi:10.7717/peerj.14461.

Weishampel, D.B., Barrett, P.M., Coria, R.A., Le Loeufl, J., Xu, X., Zhao, X., et al. 2004. Dinosaur distribution. *In* The dinosauria. 2nd ed. *Edited by* D.B. Weishampel, P. Dodson and H. Osmólska. University of California Press, Berkeley. pp. 517–606.

Wood, J.M. 1989. Alluvial architecture of the Upper Cretaceous Judith River Formation, Dinosaur Provincial Park, Alberta, Canada. Bulletin of Canadian Petroleum Geology, **37**: 169–181.

Zhang, Z., Wang, T., Ramezani, J., Lv, D., and Wang, C. 2021. Climate forcing of terrestrial carbon sink during the Middle Jurassic greenhouse climate: chronostratigraphic analysis of the Yan'an Formation, Ordos Basin, North China. GSA Bulletin, **133**: 1723–1733. doi:10.1130/b35765.1.